Nonlinear Dynamics of Passionflower Tendril Free Coils

Christina Cogdell and Paul Riechers

NCASO Spring 2012

Typical Free Coiling Patterns

Cylindrical

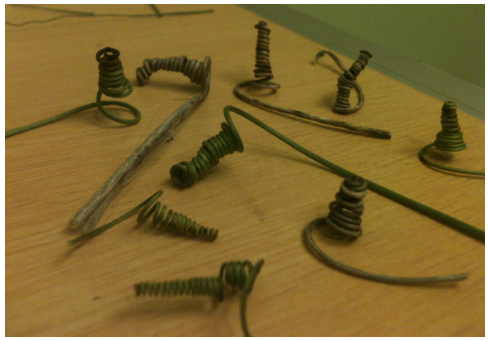

Conical

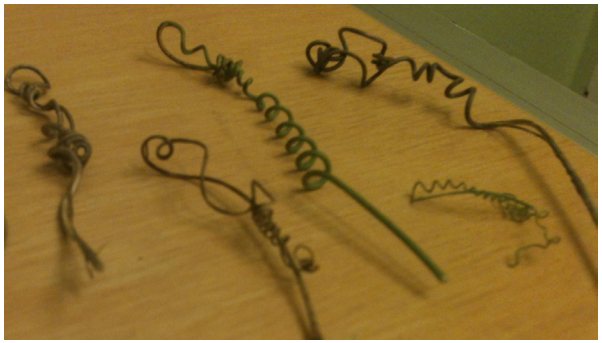

Reversals

Knots

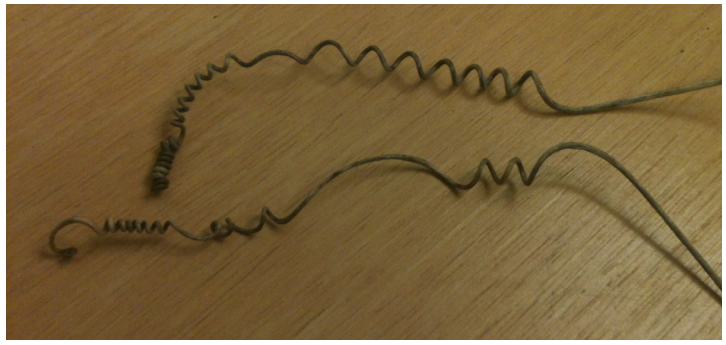

Multiple Perversions

90-degree Single Perversion

State of the Field - Common Misunderstandings about Tendril Free Coiling

1) Free coiling tendrils are *not interesting* because they (presumably) are *functionally irrelevant* to a vine if they are not supporting any weight or stabilizing the plant from environmental forces.

2) *Perversions* (which results in a shift in handedness of the coil direction) *do not happen in free coiling tendrils*. Perversions only occur in tendrils that are contact coiling while both ends of the tendril are fixed. Look up and see that this isn't true.

3) *Differential growth* is not the same process as *differential contraction and elongation* during coiling, although they share some chemical signaling, mechanical and morphological similarities.

4) *We have not found a single article whose primary subject matter is free coiling in tendrils*; the few articles about nonlinear dynamics in coiling address only contact coiling or general twining morphology in vines.

Existing Tendril Coiling Models:
Invariant Helical Contact Coils Explained Using Mechanical Models Based upon Kirchhoff's Equations for Rods with Intrinsic Curvature at Equilibria in Minimal Energy State

The Kirchhoff model of rod dynamics describes inextensible rods whose length is much greater than the cross sectional radius. Using these fundamental assumptions, all the physical quantities associated with the filament are averaged over the cross sections and attached to the central axis. The total force $F = F(s,t)$ and moment $M = M(s,t)$ can then be expressed in terms of the local basis. The conservation of linear and angular momentum leads to the Kirchhoff equations which, in scaled variables and for a rod of circular cross section, are [8]

$$F'' = \ddot{d}_3 \,, \tag{2}$$

$$M' + d_3 \times F = d_1 \times \ddot{d}_1 + d_2 \times \ddot{d}_2 \,, \tag{3}$$

$$M = (\kappa_1 - \kappa_1^{(u)})d_1 + (\kappa_2 - \kappa_2^{(u)})d_2 + \Gamma(\kappa_3 - \kappa_3^{(u)})d_3 \,. \tag{4}$$

From Alain Goriely and Michael Tabor, "Spontaneous Helix Hand Reversal and Tendril Perversion in Climbing Plants," Physical Review Letters 80:7 (16 Feb. 1998): 1564-67.

Kirchhoff's equations are used to explain the presence of one or more perversions in a coil that is fixed at both ends.

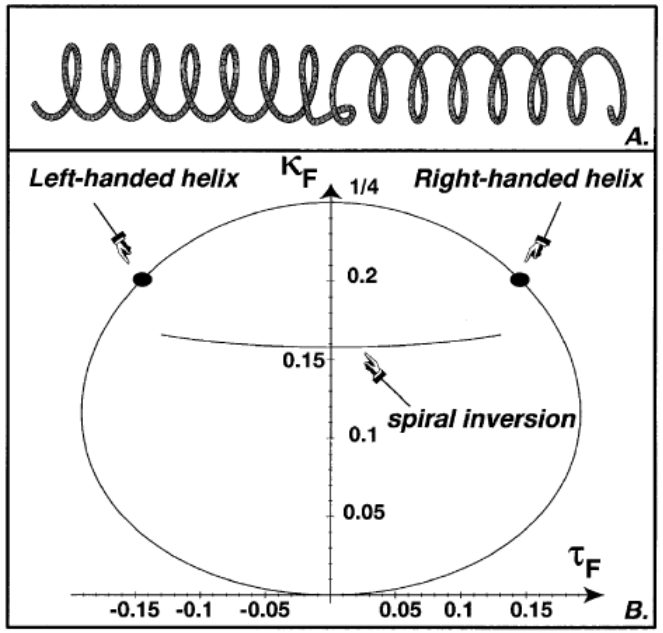

FIG. 2. (*A*) Sketch of a helix hand reversal. (*B*) The optimal solution curves in the $\tau_F - \kappa_F$ plane together with the two optimal helices (circles) obtained for $K = 1/4$, $\Gamma = 3/4$, $n = 1/8$, and $\phi = \phi_2 \approx 0.286$. The inside curve is the one obtained by the nonlinear analysis for the central piece.

How to Make an Invariant Helix: Twist + Bend

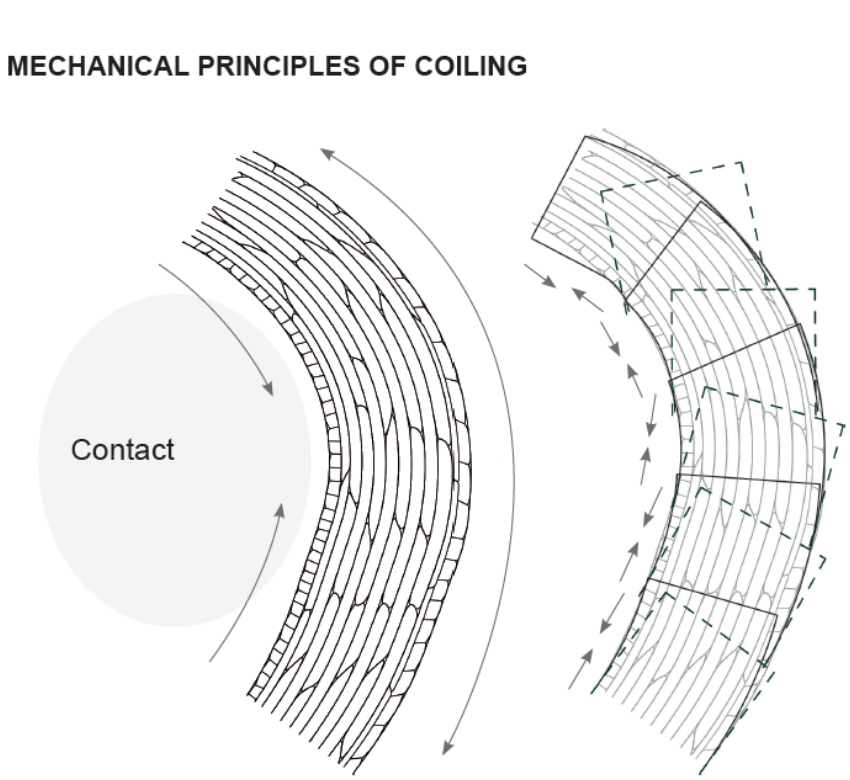

Curvature due to thigmotropism produced by differentiated elongation. Cells on the contact side contract whereas cells on the opposite side elongate.

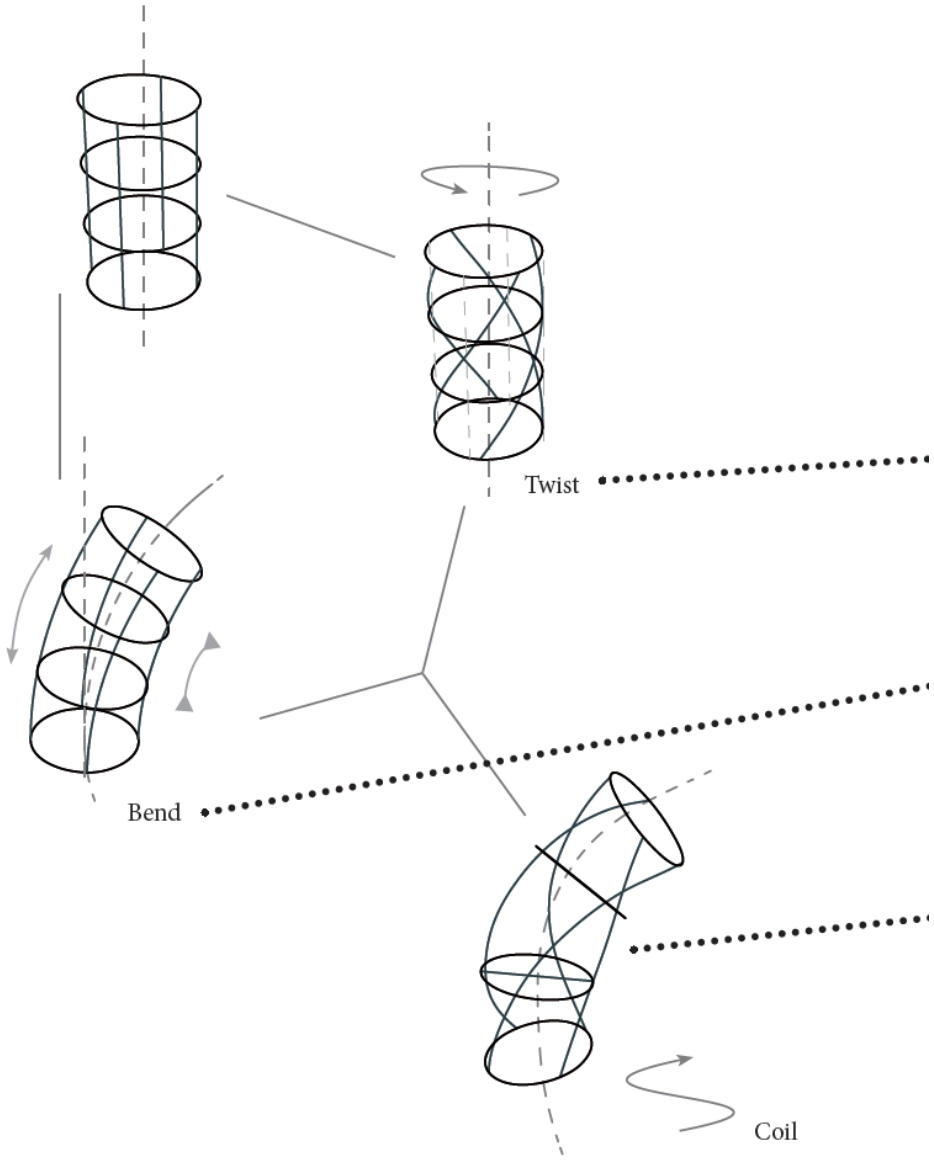

Our Method for Studying the Nonlinear Dynamics of Free Coiling

I. Create a Reasonable Interdisciplinary Hypothesis of the Biological, Chemical and Mechanical Processes that Generate Coiling:
1) Research to compile a holistic view of the major facets of the "system";
2) Use this hypothesis as the basis for a mathematical model that simulates the dynamics and patterns of free coiling.

II. Harvest and Measure 500 Free Coiling Tendrils from Christina's Passionflower Vine for Statistical Analysis Using Computational Mechanics:
1) 5mm increment per "symbol," starting at the tip of the tendril.
2) "Subsymbols" of "symbol" designate range of coil diameter [d, D, 2], periodicity [p, P, 3], handedness [L, R, S], perversions or not [0, 1], angular axis changes [4, 9, 8], self-contact or not [c, f].
3) Possible "symbols" by general large category = 81; all possible "symbols" by precise subsymbol categories = 324.

~3400 symbols overall for all 501 tendrils, circa 17 meters of total coil length measured!

tendril50= ['d3R04f', 'D3R08f', 'DPR04f']
tendril51= ['DPL04f', 'DPL04f', '2pS19f', 'DPR04f', 'DPR04f', 'DPR04f']
tendril52= ['D3L19c', 'D3R18c', 'DpL04f', 'DPL04f', 'DpS14f', 'DpR04f', 'DpR04f']
tendril53= ['2pL04f', '2pL04f', '2pL04f', '2pL04f', '2pL04f', '2pL04f', '2pL04f', '2pL08f', '2pL04f', '2pL04f', '2pL04f', '2pL09f', '2pL04f', '2pL09f']
tendril54= ['d3R19f', 'DPL04f', 'DPL04f', 'DPL04f', 'DpS14f', '2pS14f', 'DpR04f', 'DpR04f', 'DpR04f', 'DpR04f', 'DpR04f', 'DpR04f']
tendril55= ['dpL04f', 'D3L04f', '2pS14f', '2pS18f', '2pR04f']
tendril56= ['DPL04f', 'D3L08f', 'DPL04f', 'DPL04f']
tendril57= ['d3R18c', 'd3L04f', 'd3L04f', 'DPL04f', 'DpL04f', 'DpL04f']
tendril58= ['D3R19c', 'd3L04f', 'D3L04f']
tendril59= ['2pS04f', '2pS04f', '2pS04f', 'DPR04f', 'DPR04f', 'DPR04f', 'DPR04f']

III. Use Python Scripting and Computational Mechanics to Create Epsilon-Machines for the Real Tendril Data

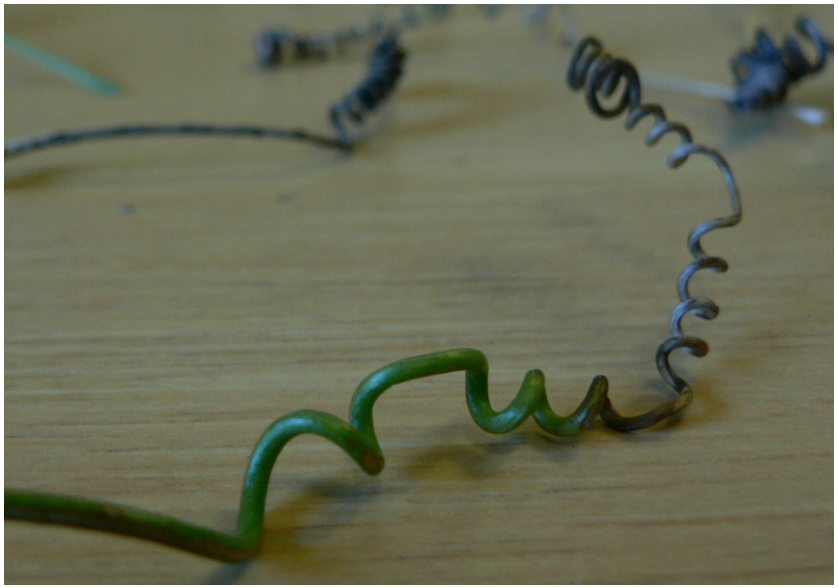

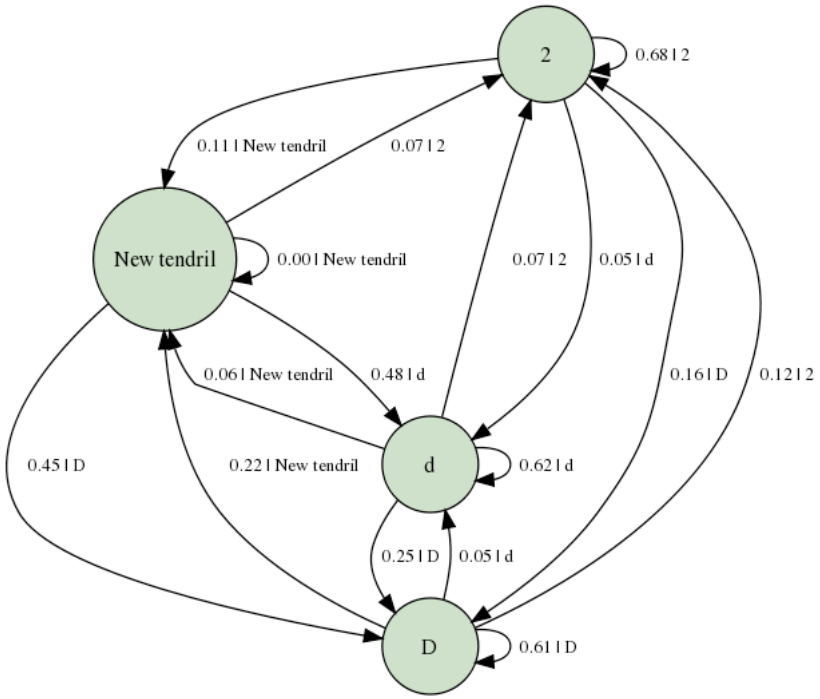

IV. Use our Mathematical Model to Generate Simulated Free Coils and Analyze the Simulated Tendrils using Computational Mechanics to Create Epsilon-Machines for the Simulated Tendrils

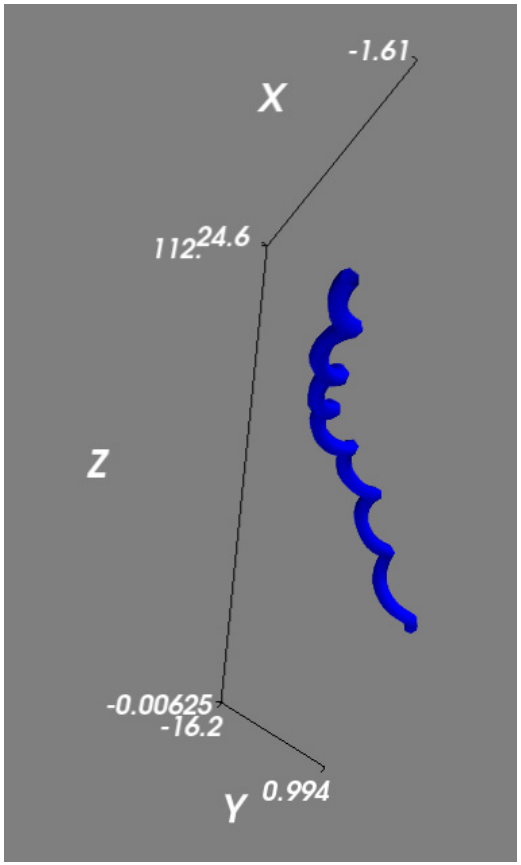

First Simulated Variant Helix Generated Using
Turing's Reaction-Diffusion Equations

V. Compare the Epsilon-Machine Results for the Real and the Simulated Tendrils to Ascertain the Strengths and Weaknesses of our Method and the General Accuracy via Predictability of Tendril Free Coiling Dynamics, Based Upon our Hypothetical Biological System and its Corresponding Mathematical Model.

Tendril Growth and Coil Patterning - Other Views on the Vine

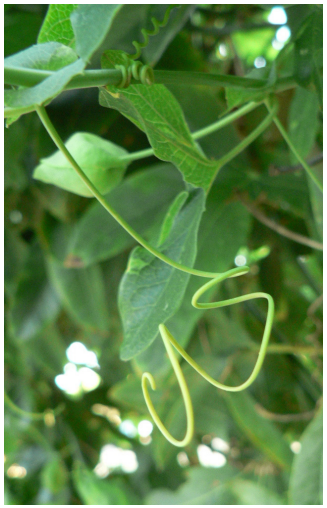

0504 6;30am Growing with a Perversion

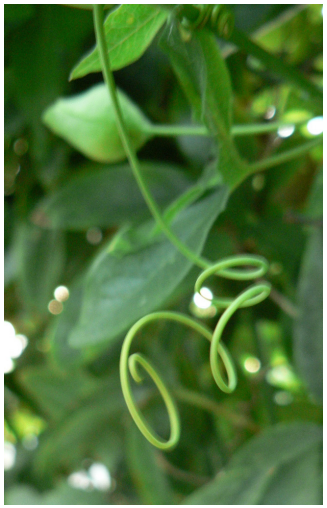

0504 1:20pm

0505 12:00pm

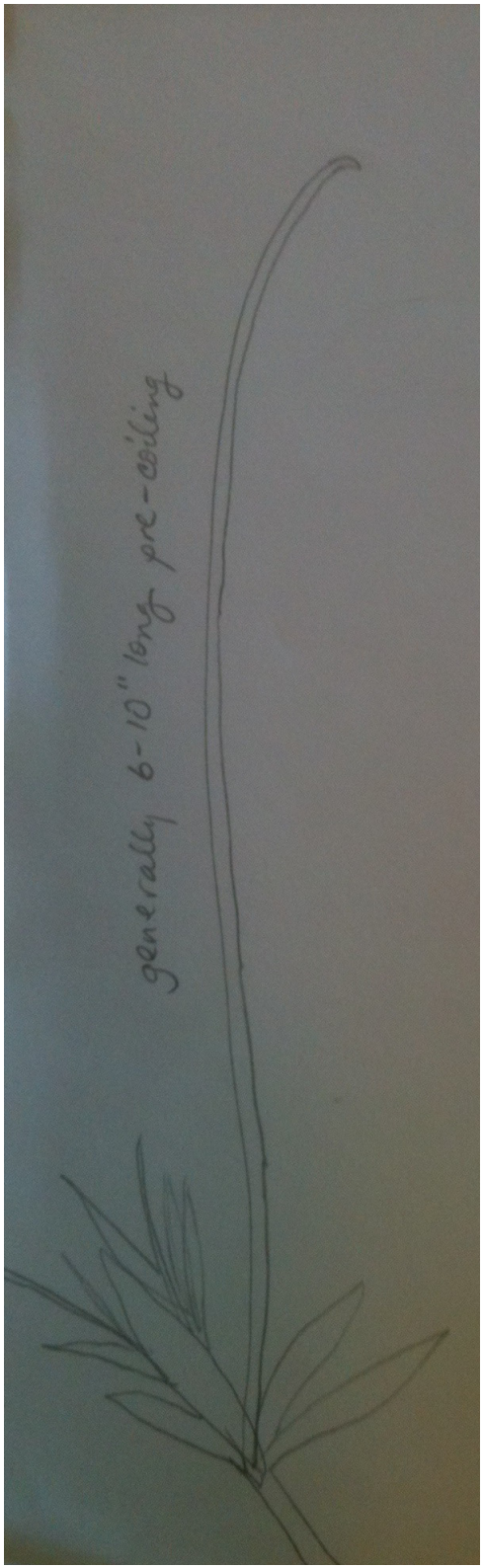

General Diagram of Bidirectional Coiling Tendril Tissue

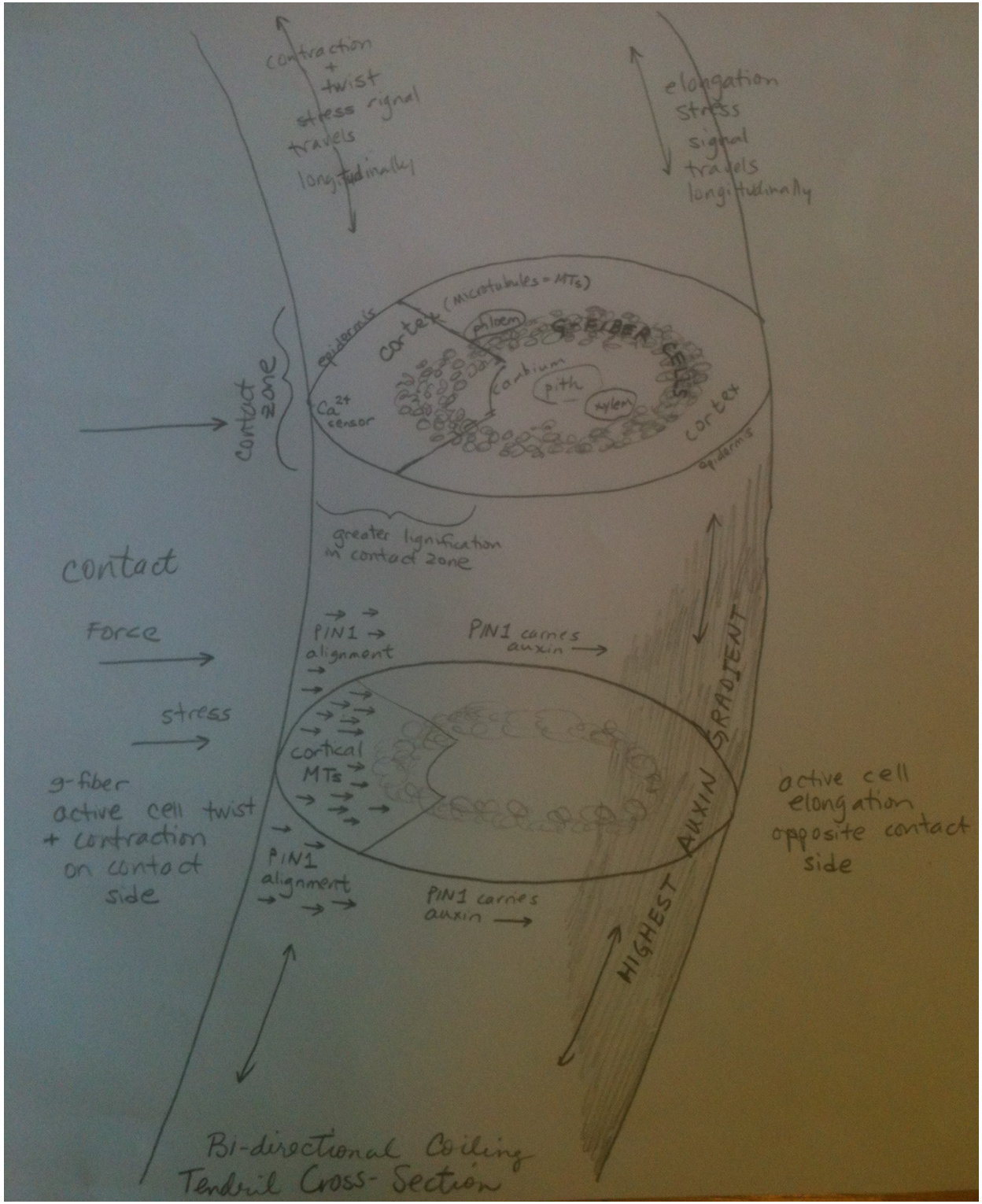

Working Hypothesis of Tendril Coiling Process:
Step 1 - Auxin Triggers Cell Elongation on Convex Side of Coil

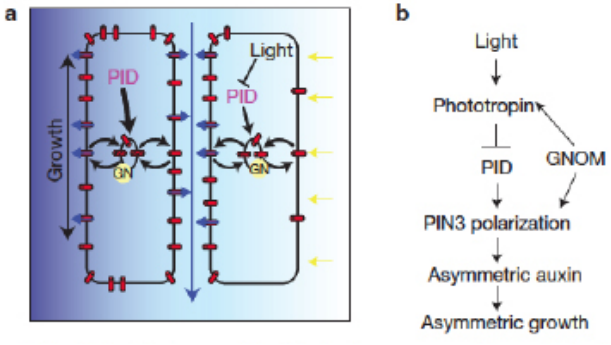

Above: Phototropic response showing PIN3 polarization carrying auxin to side opposite light toward greatest auxin concentration, where it triggers cell elongation causing the plant to curve and grow toward the light. From Ding, Zhaojun et al, "Light-mediated polarization of the PIN3 auxin transporter for the phototropic response in Arabidopsis," Nature Cell Biology 13:4 (April 2011): 447-53.

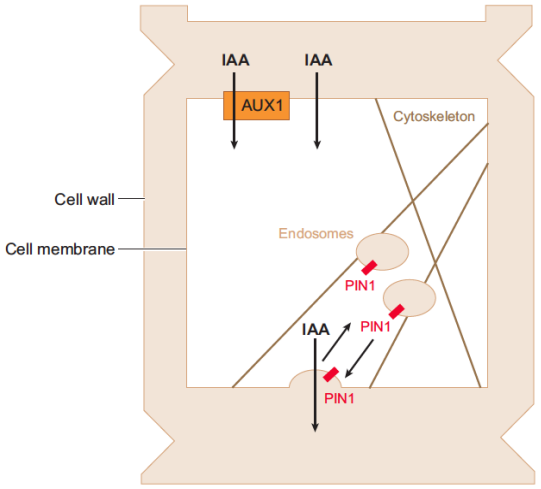

Left: Diagram showing auxin diffusion into a cell and active transport out of the cell via PIN1. From Benjamin, Rene, and Ben Scheres, "Auxin: The Looping Star in Plant Development," Annual Review of Plant Biology 59 (2008): 443-65.

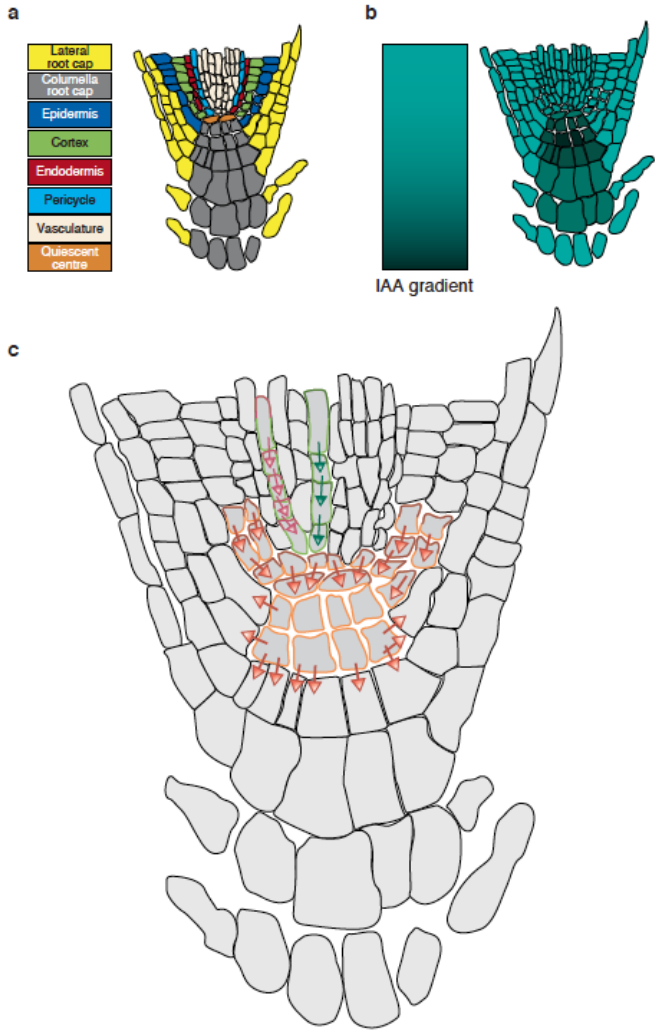

Above: Diagram showing auxin gradients and polar auxin transport in *Arabidopsis* root apex. From Bhalero, Rishikesh and Malcolm Bennett, "The case for morphogens in plants," Nature Cell Biology 5:11 (November 2003): 939-42.

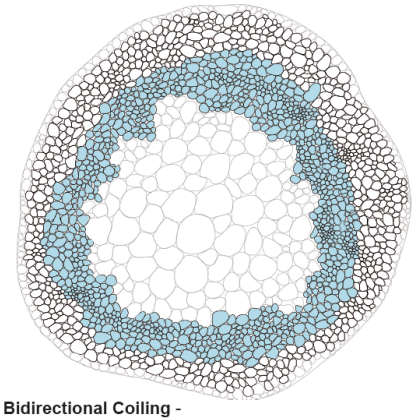

Bidirectional Coiling -
Coiling in either a clockwise or counterclockwise direction is achieved by a symmetrical cylindrical layout of gelatious fibres (g-fibre) (blue cells in above diagram) around the center of tendril. After coiling, the g-fibre uses lignification to stabilise the volume of elongated side.

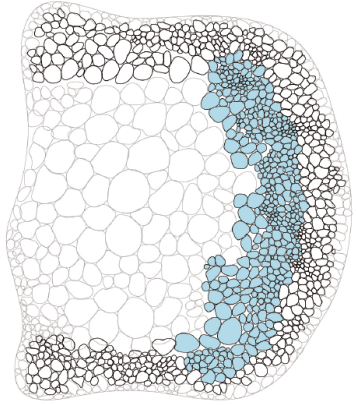

Unidirectional Coiling -
Coiling in only one direction is achieved by an asymmetrical g-fibre array (blue cells) on only one side of
the tendril.

Step 2: Role of the Gelatinous Fiber Layer in Tendril Contraction on the Concave Side of the Coil

G-fiber action in G-fiber cells causes contraction and twisting. For bidirectional coiling tendrils, there is a cylinder of G-fiber cells around the tendril, responsive to touch from any side. Only a portion on the contact side become active, whereas auxin causes cell elongation on the side opposite contact.

G-Fiber cells have 3 cell wall layers: Primary, S1 secondary, and S2 secondary, each of which has cellulose microtubules (MTs) that provide structural support. The alternating orientation of MTs is key to cell deformation patterns under G-fiber action.

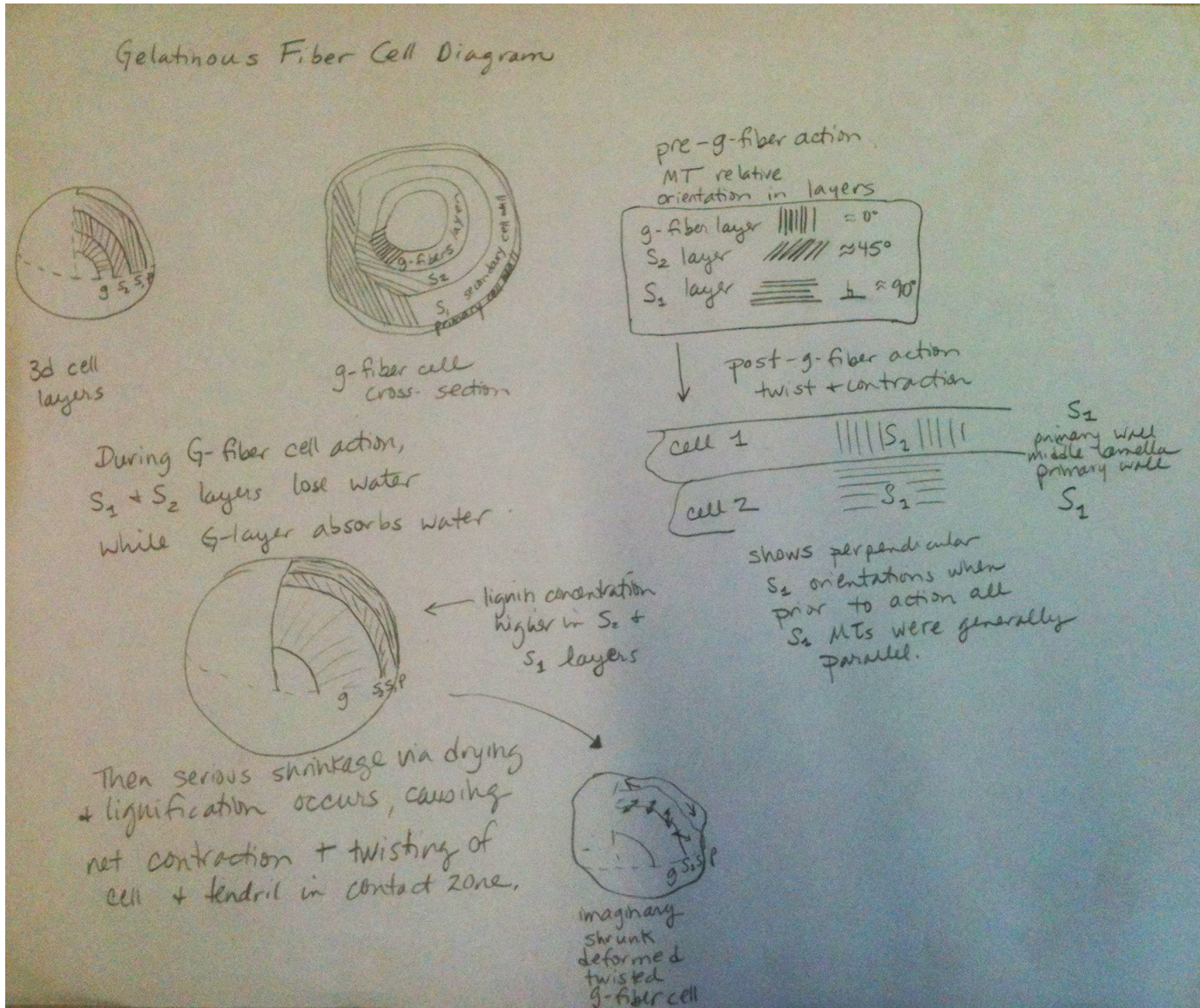

Hypothetical Model of the Process of Tendril Coiling:
G-Fiber Contraction on Contact Side + Oppositional Auxin Gradient-Induced Cell Elongation

Contraction and Twist from G-Fiber Action on Contact Side (Concave Side)

Contraction Mechanical Stress Travels Longitudinally Up and Down the Concave Side from G-Fiber Contraction + Differential Lignification for Variable Stiffening

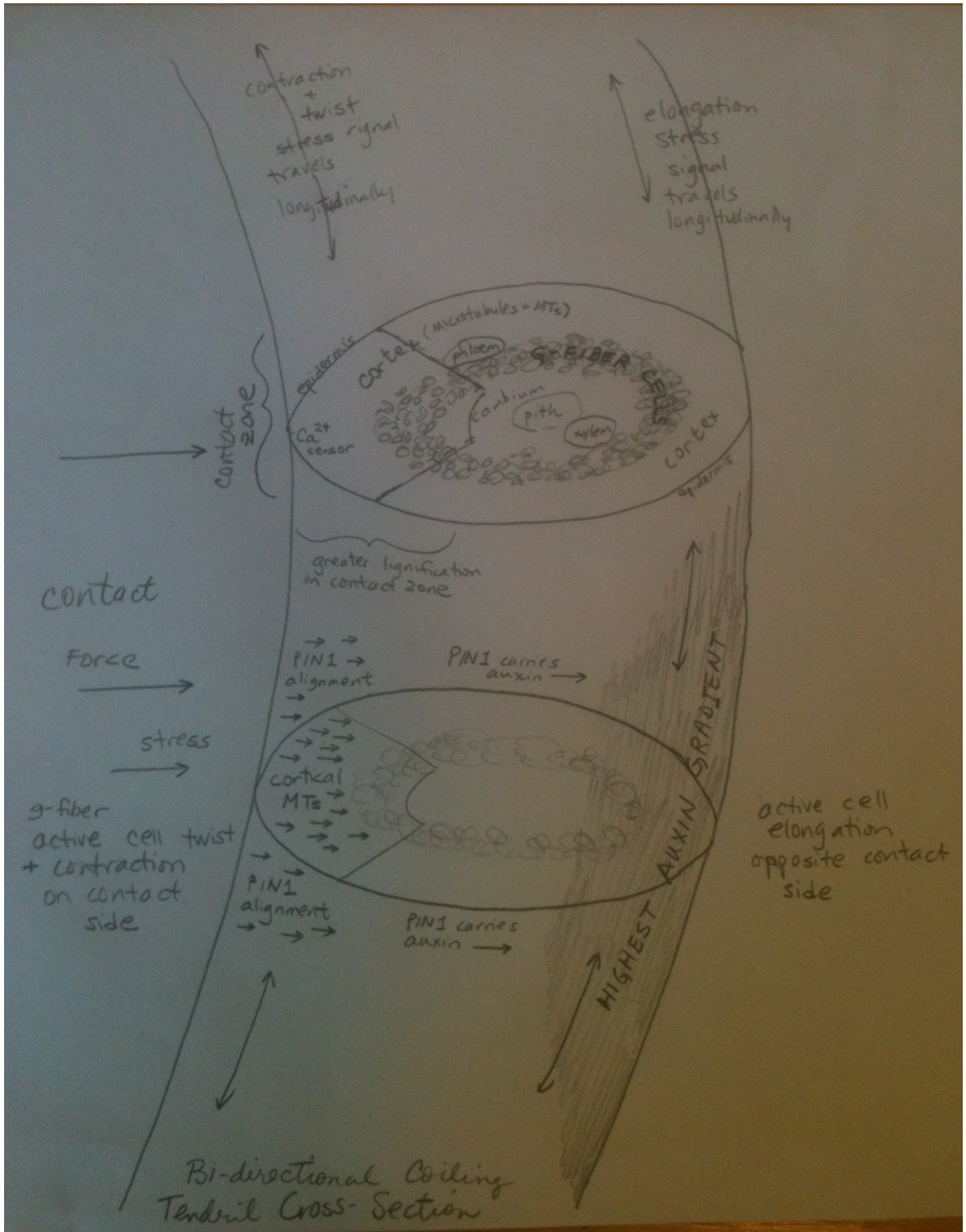

Cell Elongation from High Auxin Levels on Side Opposite Contact (Convex Side)

Elongation Mechanical Stress Travels Longitudinally Up and Down the Convex Side from Auxin-Induced Elongation

Nonlinear Coiling Pattern Dynamics: Consistent Structural Form + Stochastic Variability

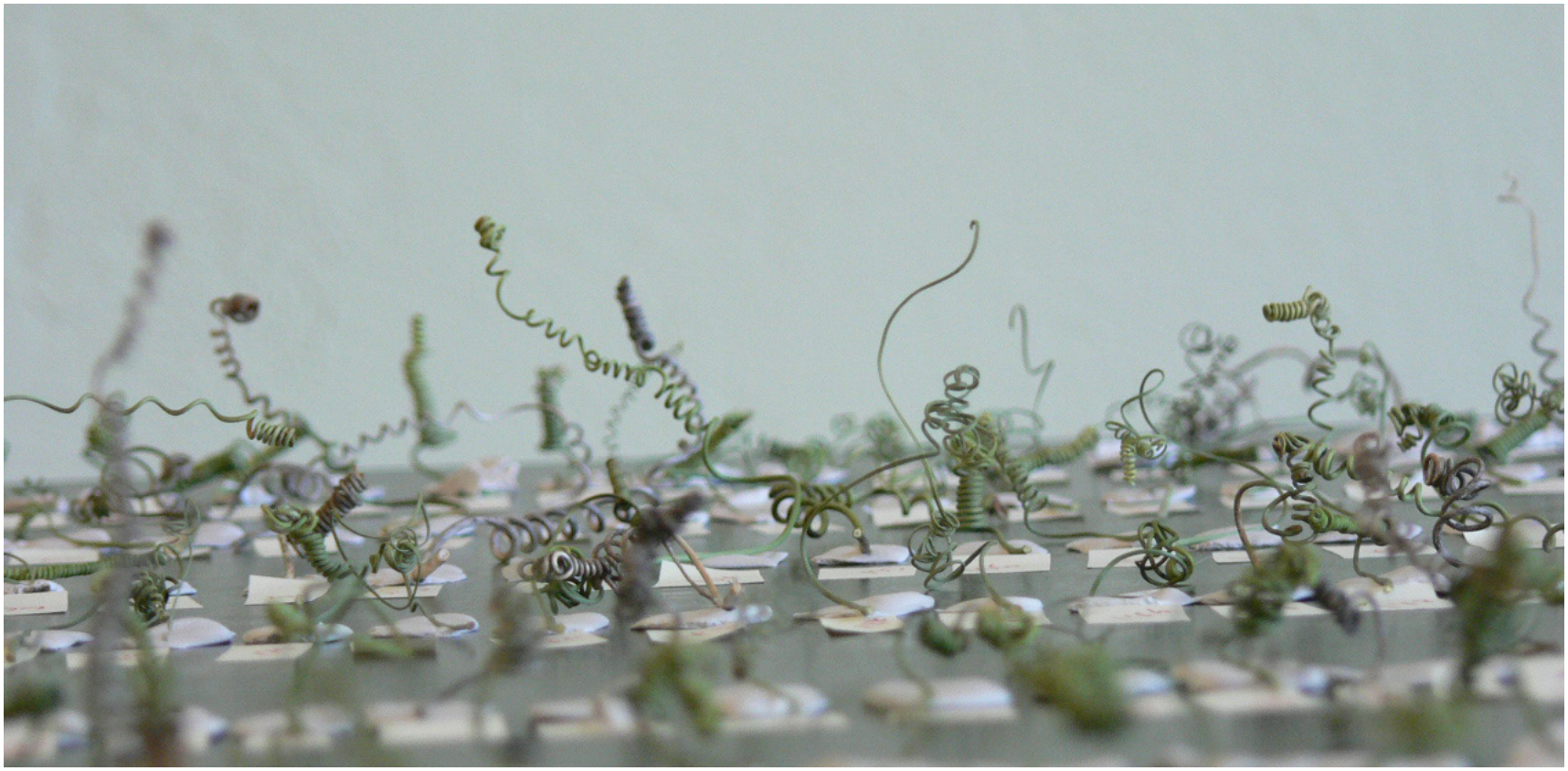

What Might Account for these Dynamics?

1) Multiple contact locations with simultaneous or temporally delayed coiling processes at work on the same tendril that have to negotiate each other;

2) Variations in lignification across the region of the contact zone of active g-fibers may cause variations in coiling diameter, angle, and periodicity;

3) Perversions may be caused by two simultaneous coiling processes on the same tendril meeting, by self-contact where the tip of the tendril becomes fixed to itself, and perhaps also by a PIN polarity reversal that shifts auxin-triggered cell elongation to the opposite side of the tendril;

4) Variations in the auxin gradient on the elongating side of the tendril may cause proportionally greater or lesser elongation (in a similar fashion to how variations in lignification on the contact side are also affecting the coiling pattern).

Understanding the Nonlinear Dynamics of Tendril Free Coiling via Computational Mechanics
Statistical Analysis of Real Tendril Morphologies

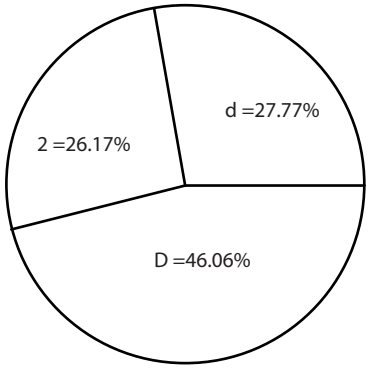

d = 0-2.99 mm
D = 3-7.99 mm
2 = > 8mm

Shannon Entropy
$H(D)$ = 1.53457054378 bits

Diameter

d

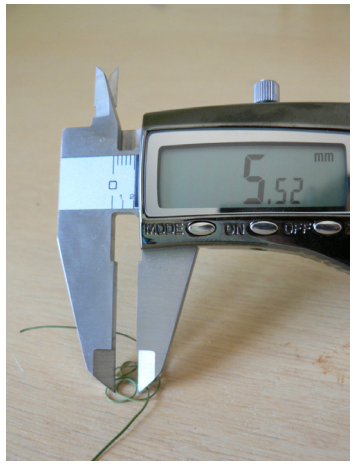

D

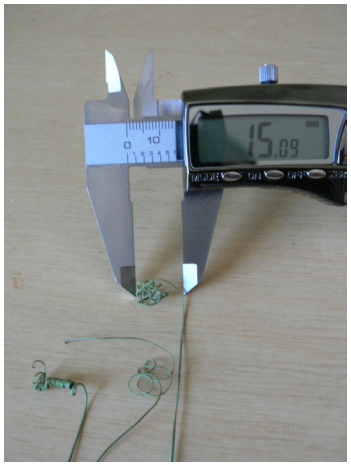

2

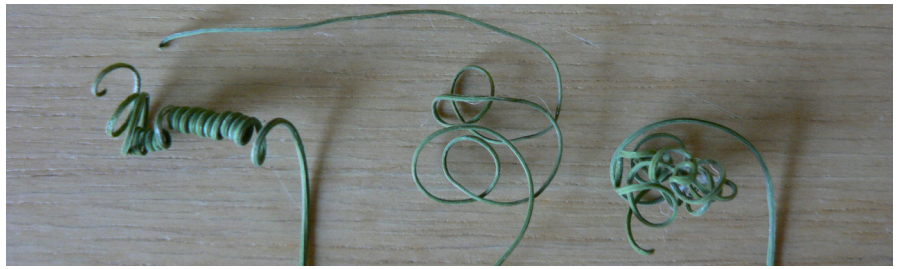

d D 2

First Order Markov Chain for Diameter

This maps the probability of seeing any subsymbol given knowledge of only the preceding subsymbol.

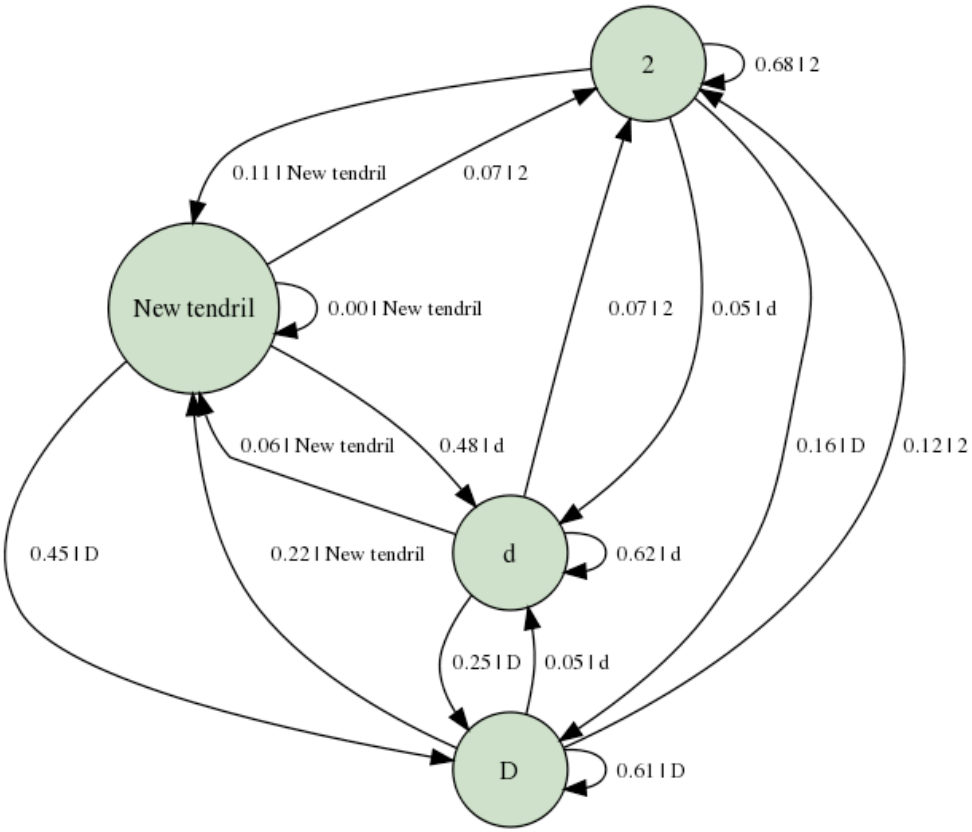

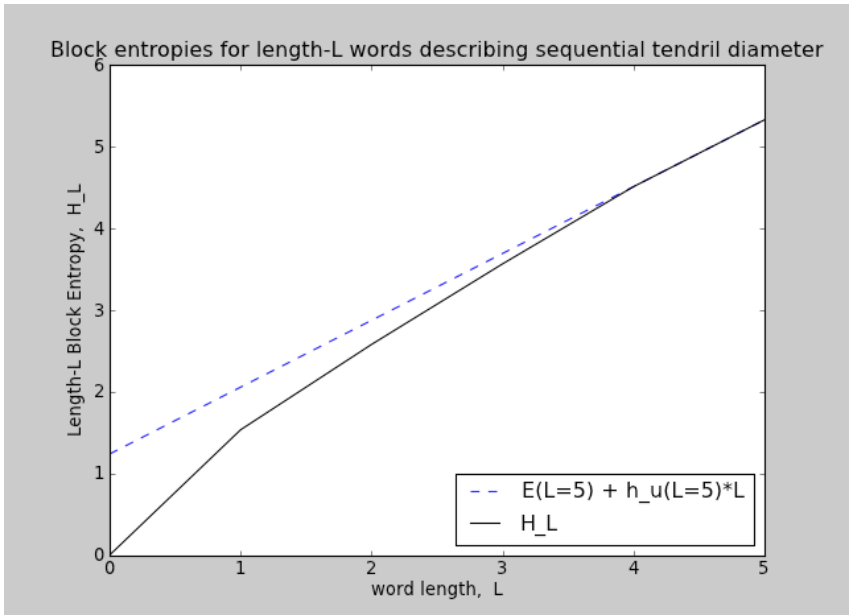

Periodicity (# of Coils/5mm)

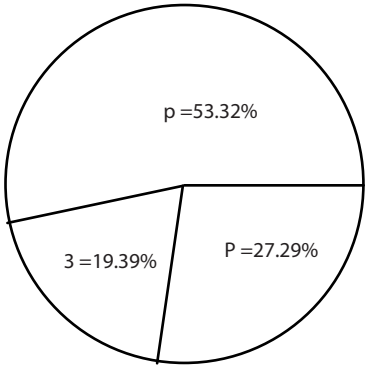

p = 0-1 coil
P = 1-4 coils
3 = > 4 coils

p

P

3

Shannon Entropy
$H(P)$ = 1.45391217496 bits

First Order Markov Chain for Periodicity

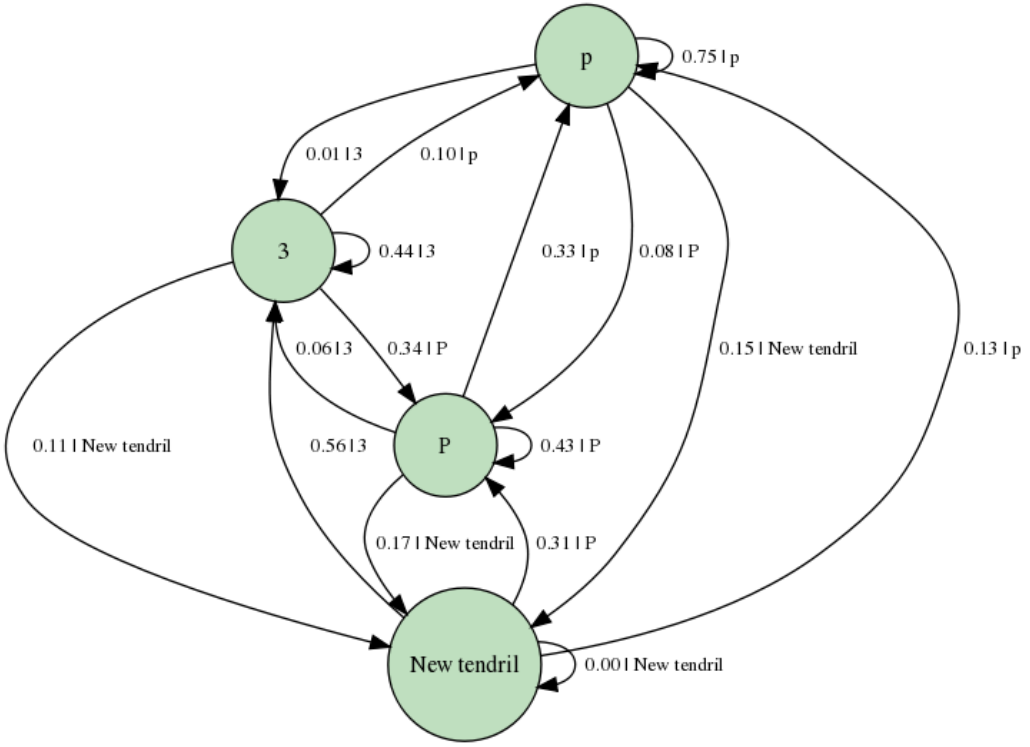

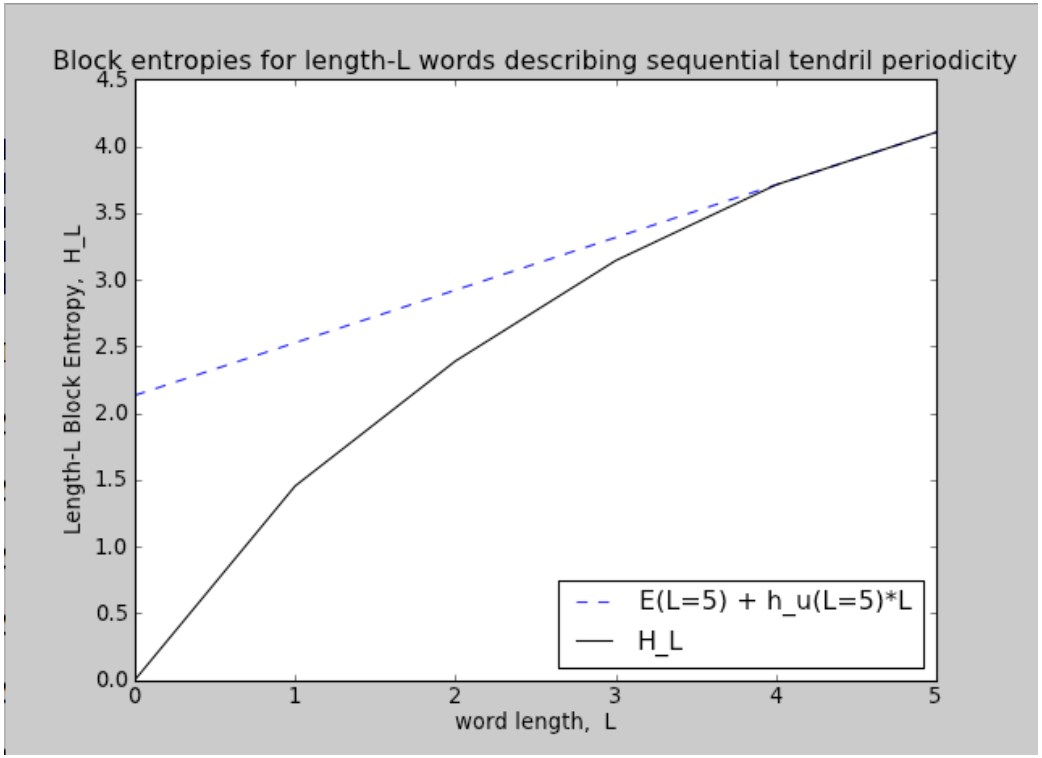

Handedness

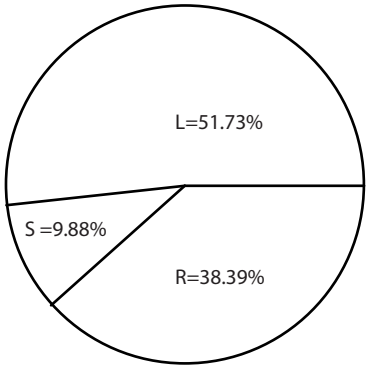

L = Left (Counterclockwise)
R = Right (Clockwise)
S = Straight (in a Perversion)

Tip Starts Left

L

Tip Starts Right

R

Straight in the middle of a perversion

S

First Order Markov Chain for Handedness

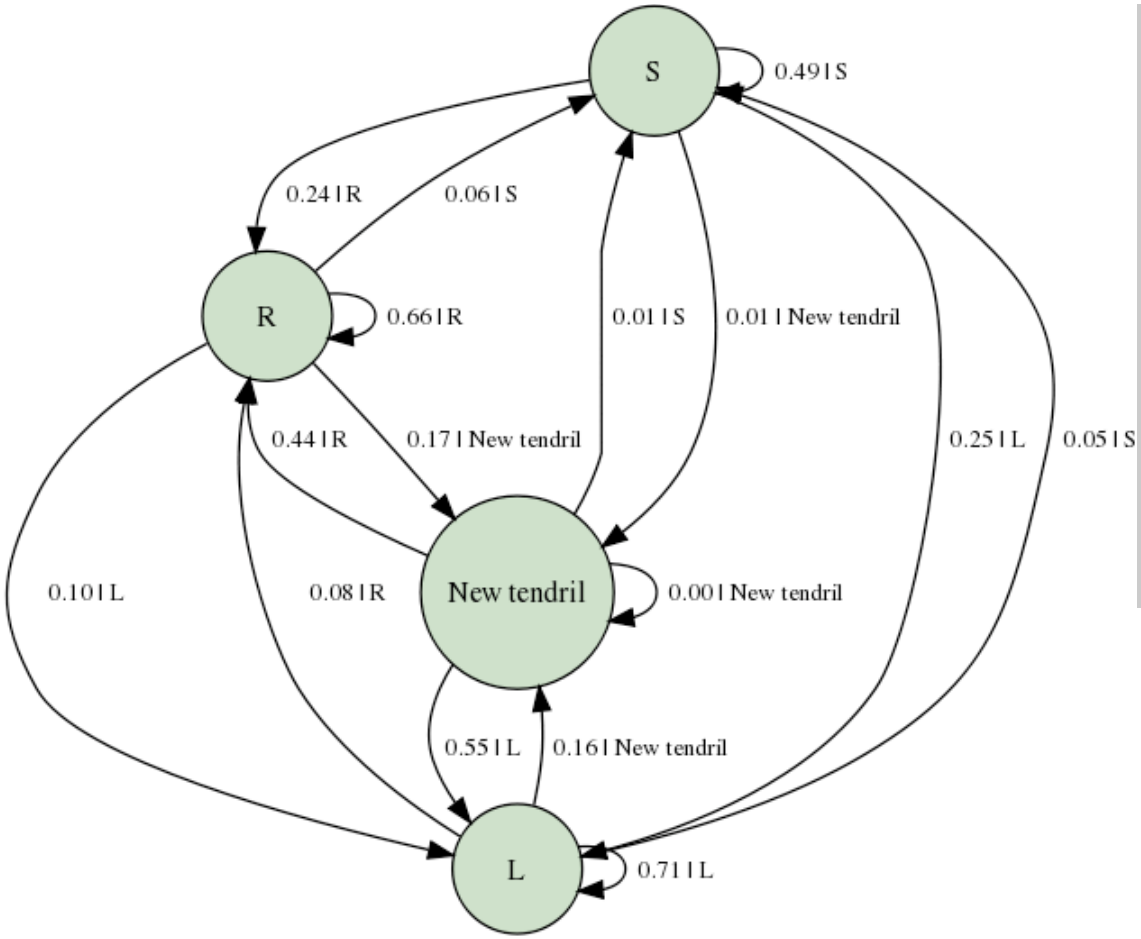

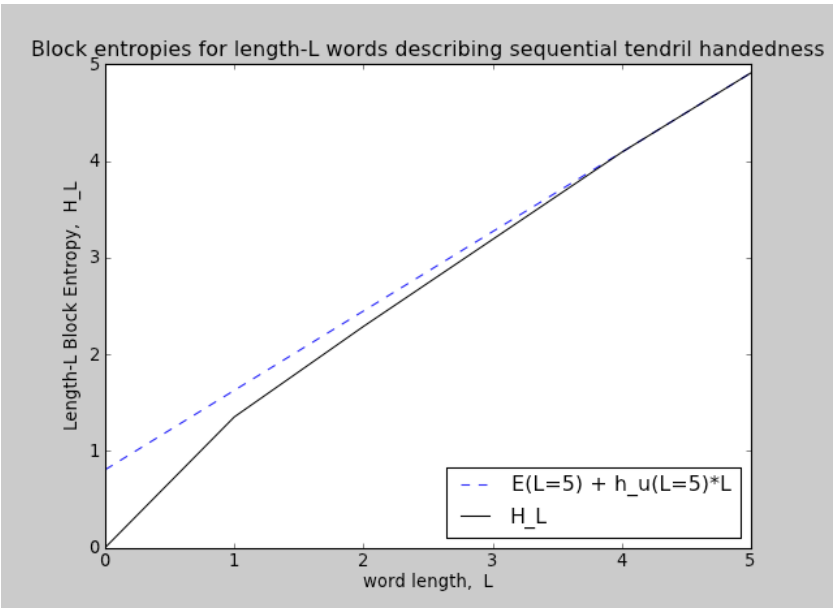

Pervertedness

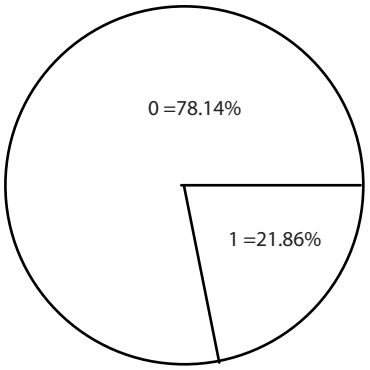

0 = No Perversion
1 = Perversion
A perversion occurs when a coil changes its handedness/directionality.

Shannon Entropy
H(Perv) = 0.757692140763 bits

0 1 0

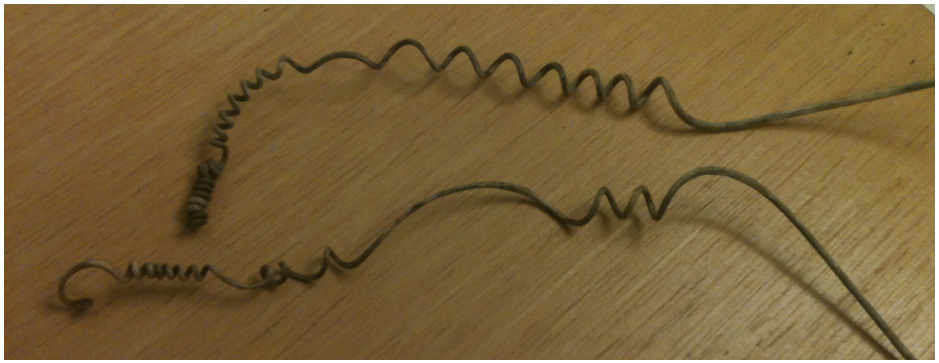

1 0 1 1 1 0

"1" gets repeated if the perversion falls into more than one measurement, so consecutive ones may imply either the same perversion and it's long, or multiple perversions back to back. If the handedness changes on either side of the perversion, this means there was an odd number of perversions. If the handedness is the same on both sides of the perversion, then there's an even number of perversions.

First Order Markov Chain for Pervertedness

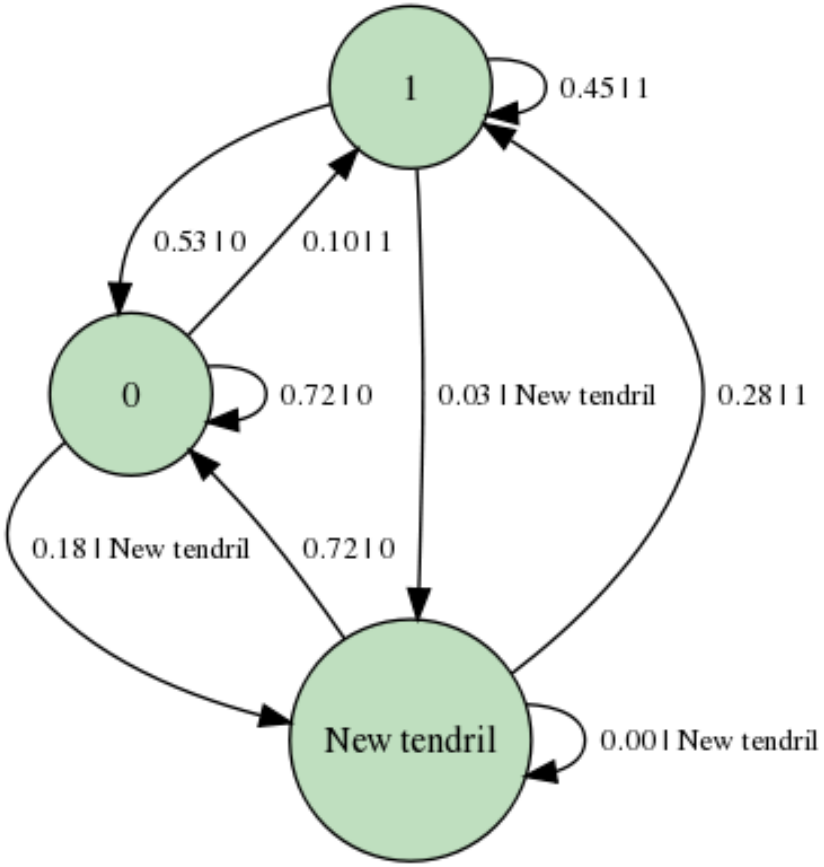

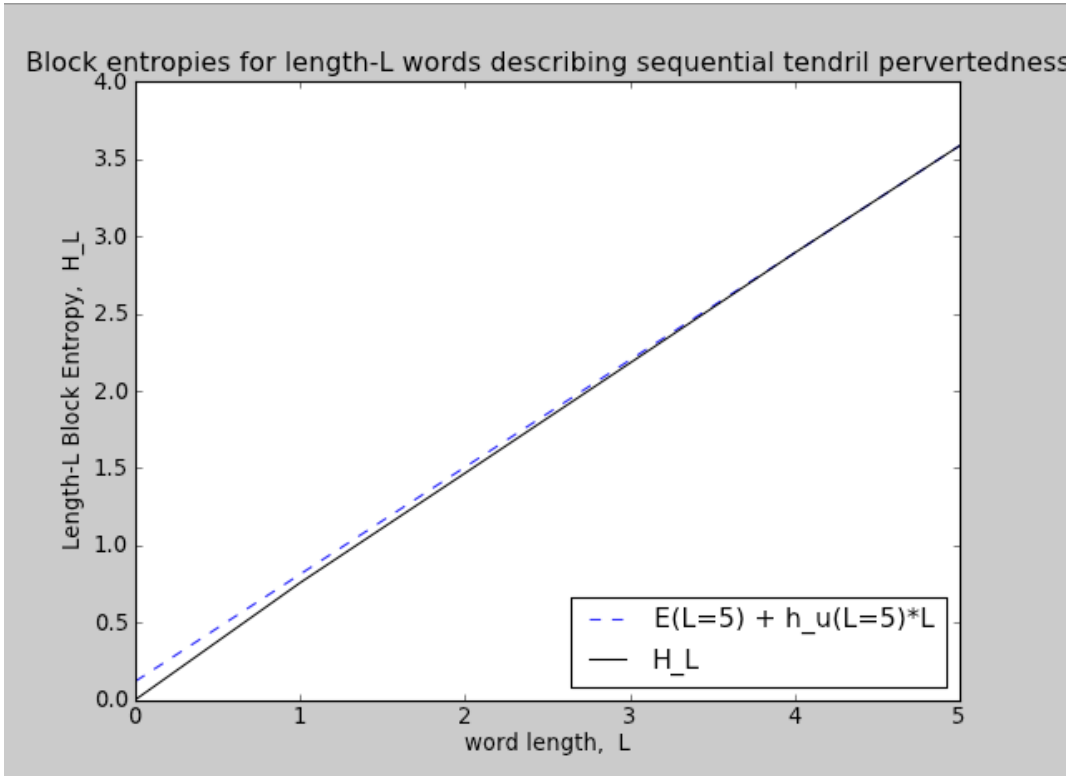

Angular Axis Rotation

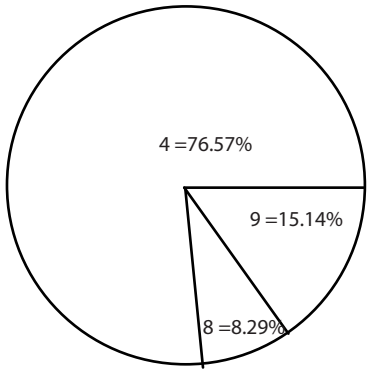

4 = 0-44.99 degrees
9 = 45-90 degrees
8 = 180 degree reversal

Shannon Entropy
$H(A)$ = 1.00505665524 bits

4

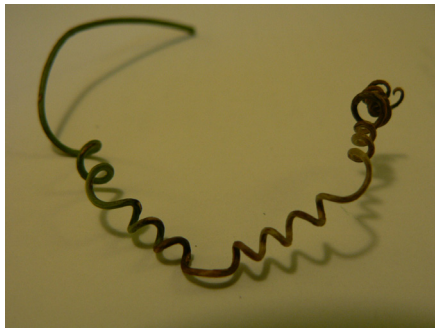

9

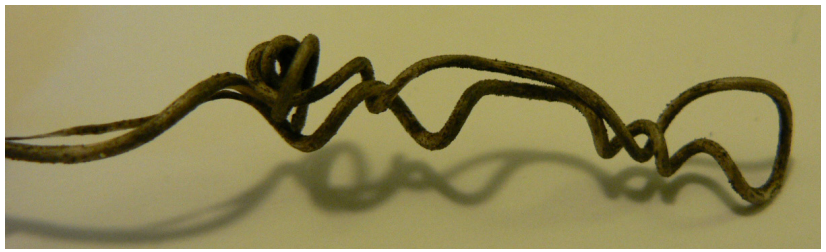

9

8

First Order Markov Chain for Angular Axis Rotation

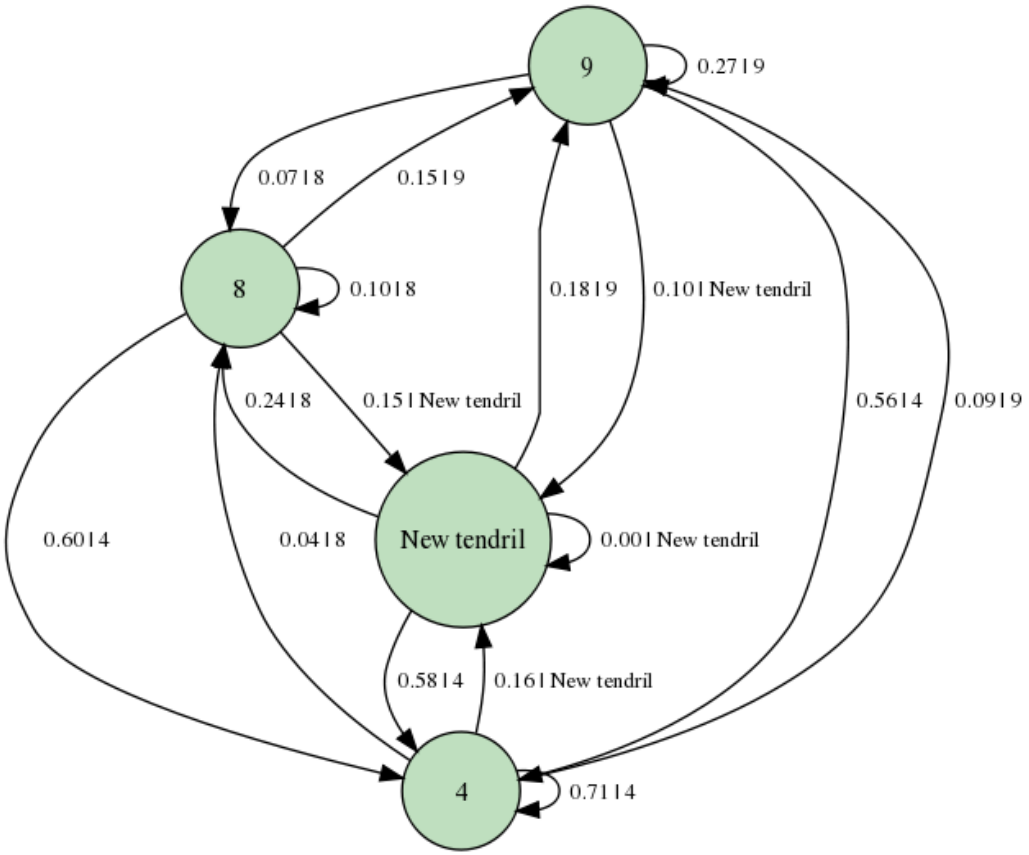

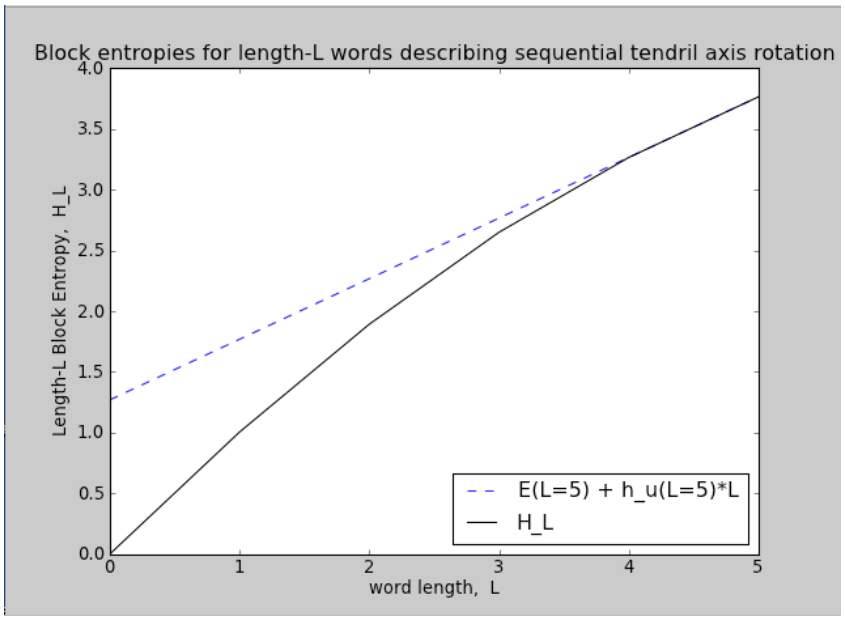

Contact Status

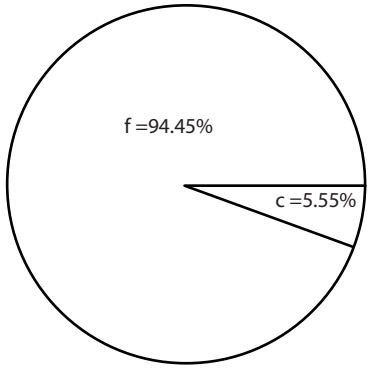

c = self-contact
f = free

f

c

c

Shannon Entropy
H(C) = 0.309208309792 bits

First Order Markov Chain for Contact Status

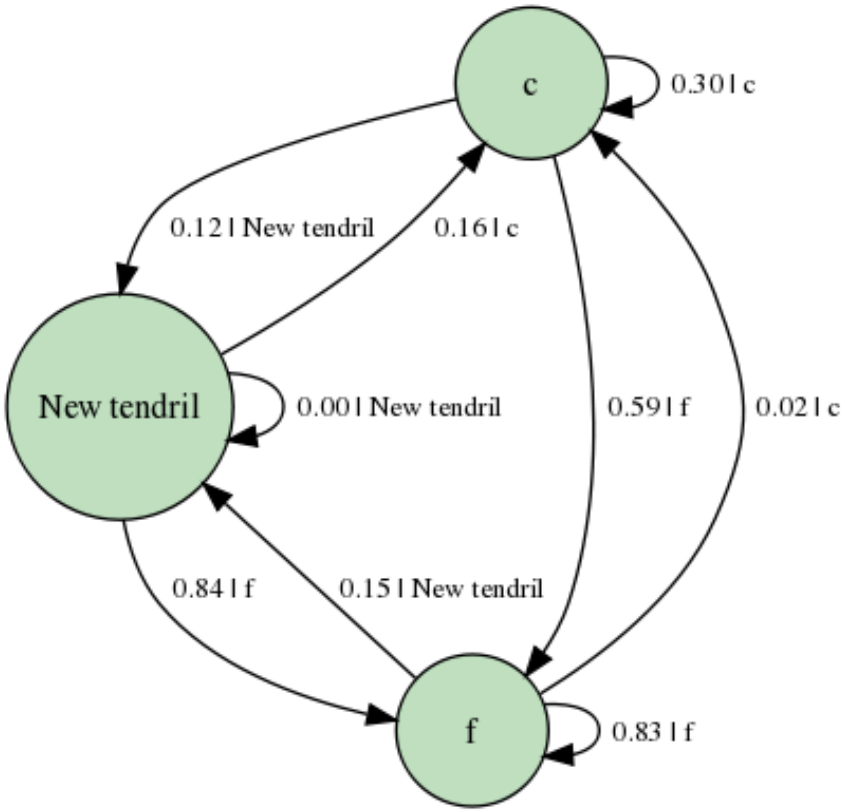

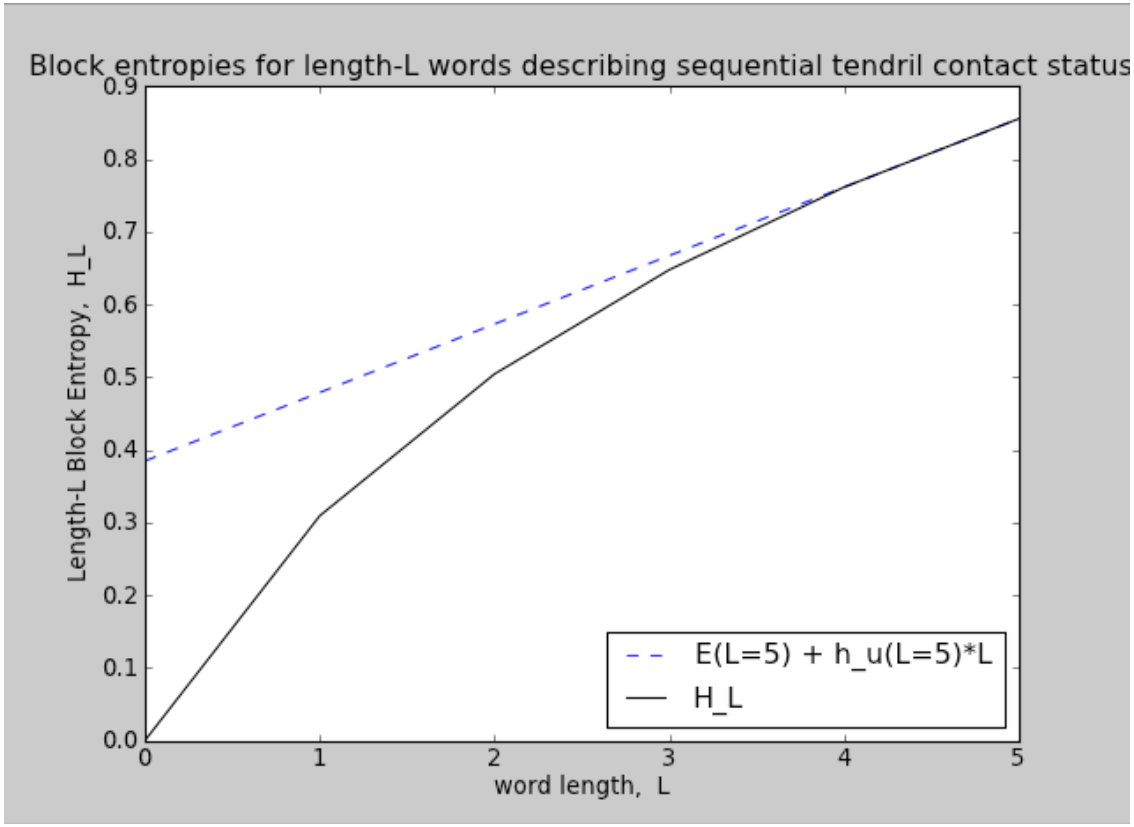

First Epsilon-Machines

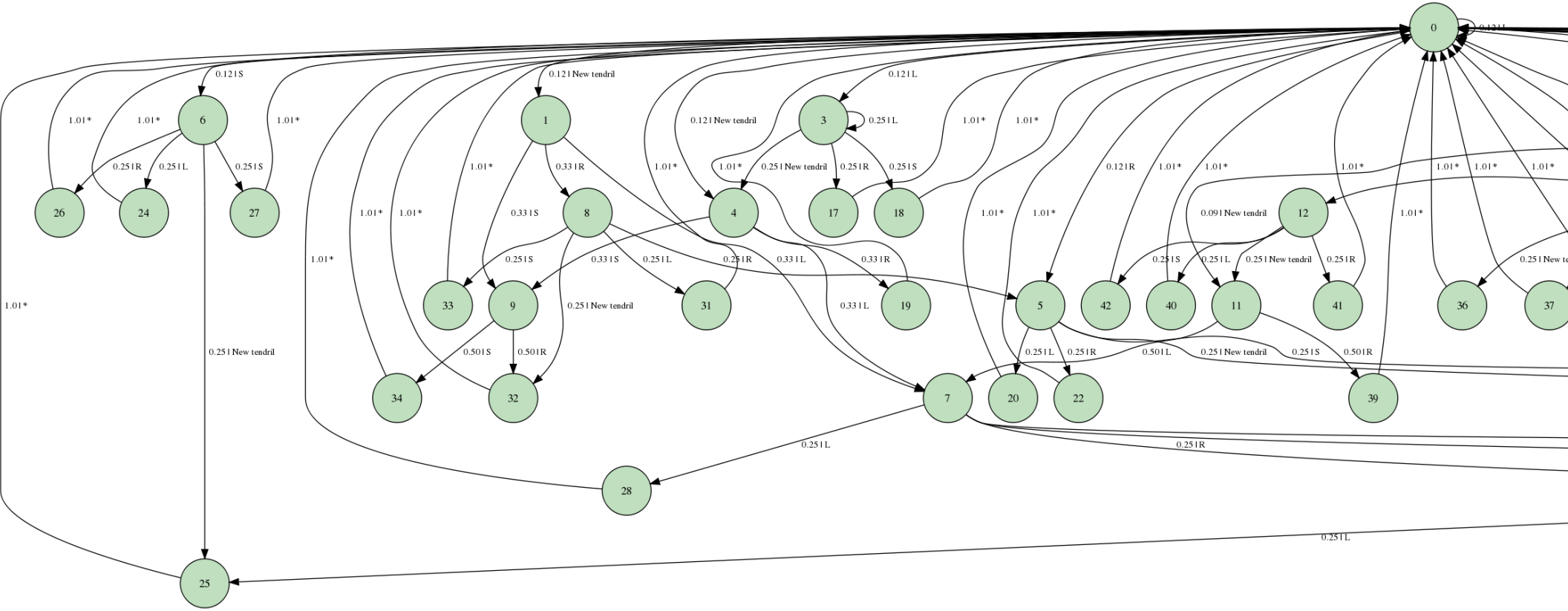

Unifilar E-Machine for Subsymbol Handedness (Left, Right, Straight), Morph Length 2 **(continued on next page)**

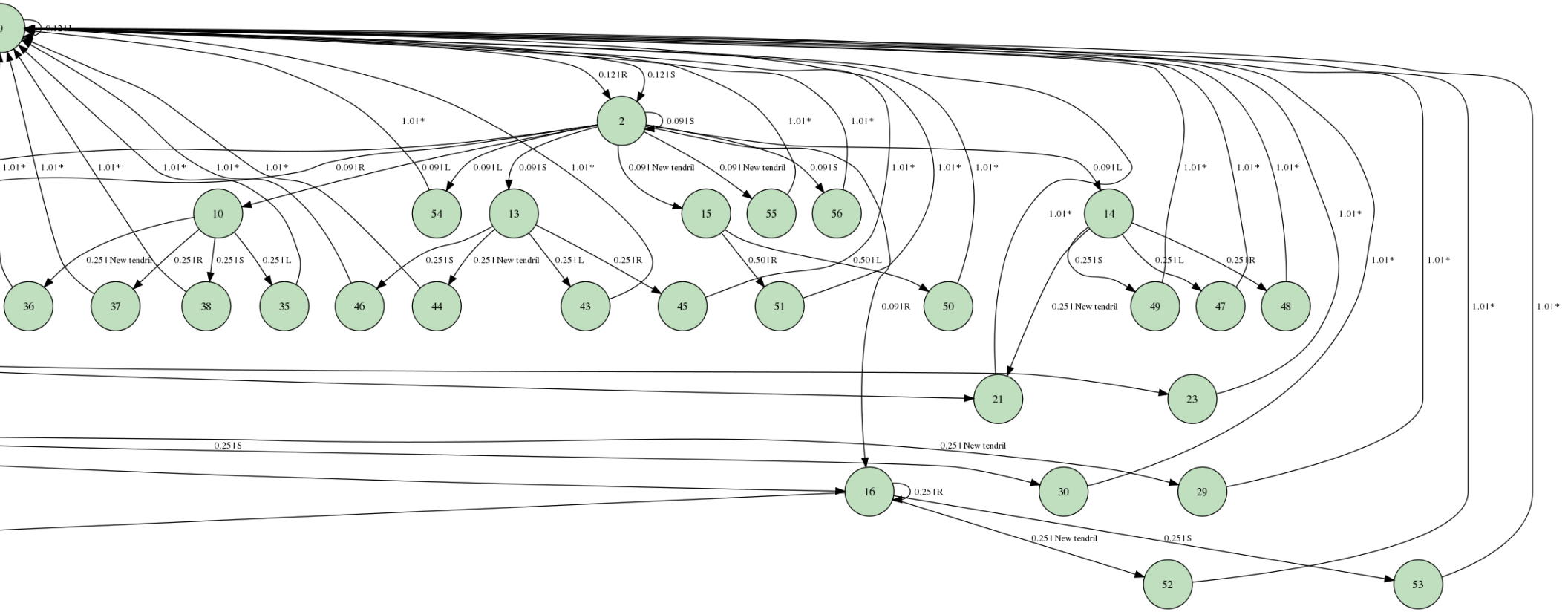

Unifilar E-Machine for Subsymbol Handedness (Left, Right, Straight), Morph Length 2 (continued from previous page)

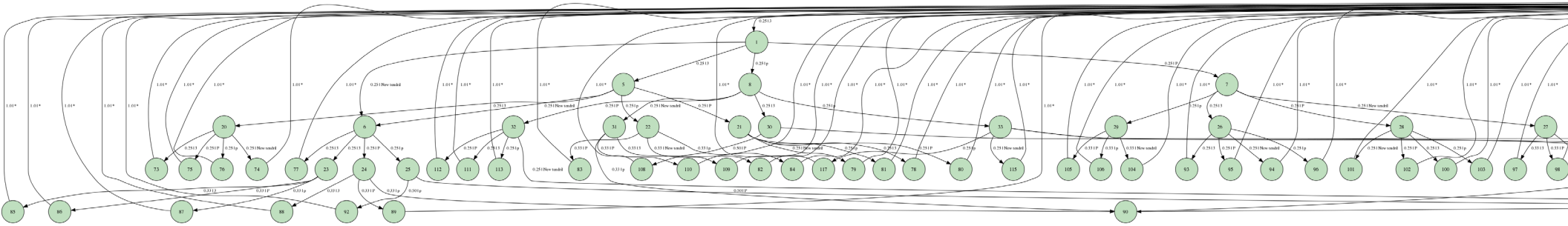

Unifilar E-Machine for Subsymbol Periodicity (“p”, “P”, “3”), Morph Length 2 (continued on next three pages!)

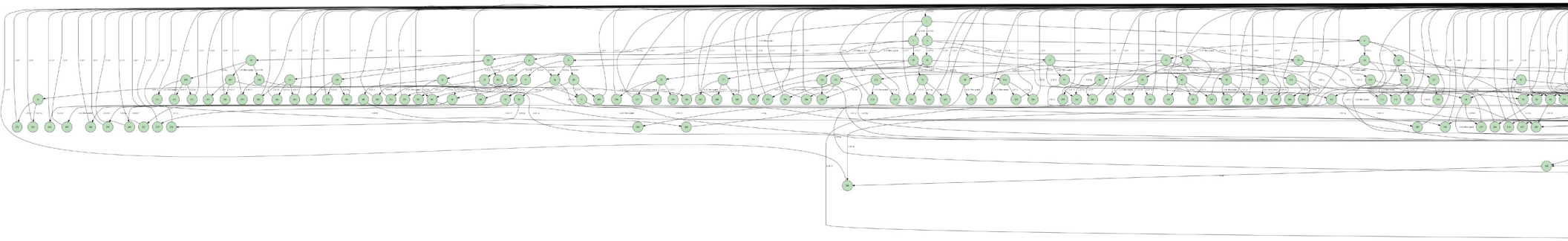

Unifilar E-Machine for Subsymbol Periodicity (“p”, “P”, “3”), Morph Length 4 (continued on next three pages!)

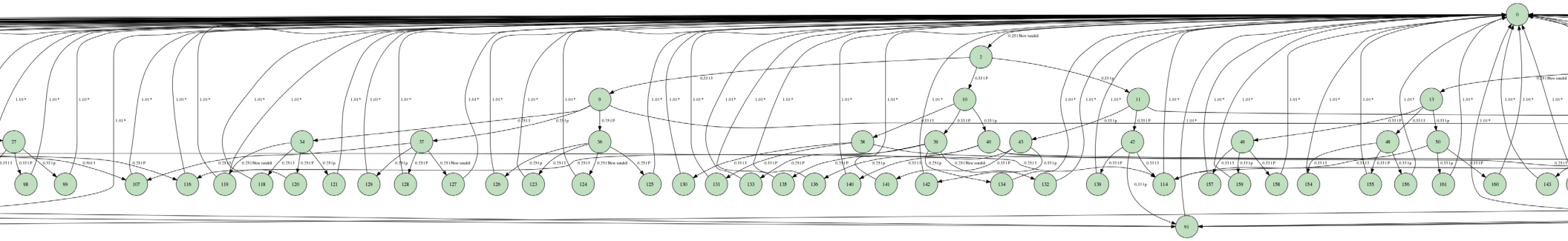

Unifilar E-Machine for Subsymbol Periodicity (“p”, “P”, “3”), Morph Length 2 (continued on next two pages!)

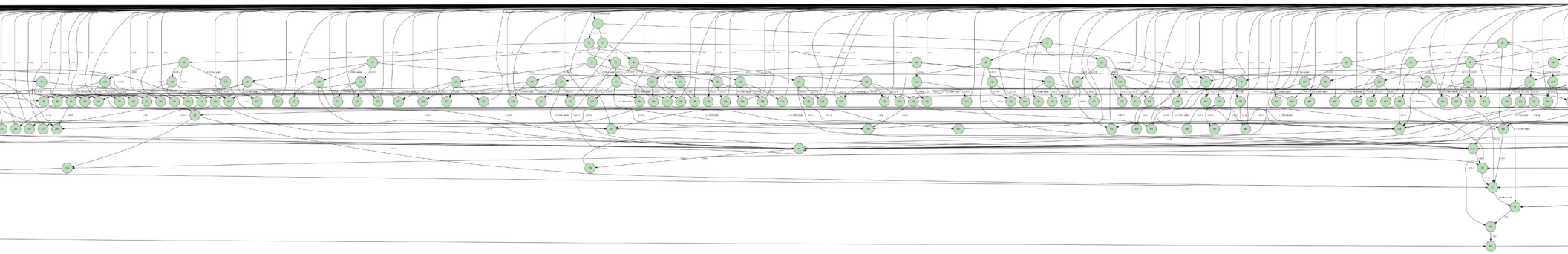

Unifilar E-Machine for Subsymbol Periodicity (“p”, “P”, “3”), Morph Length 4 (continued on next two pages!)

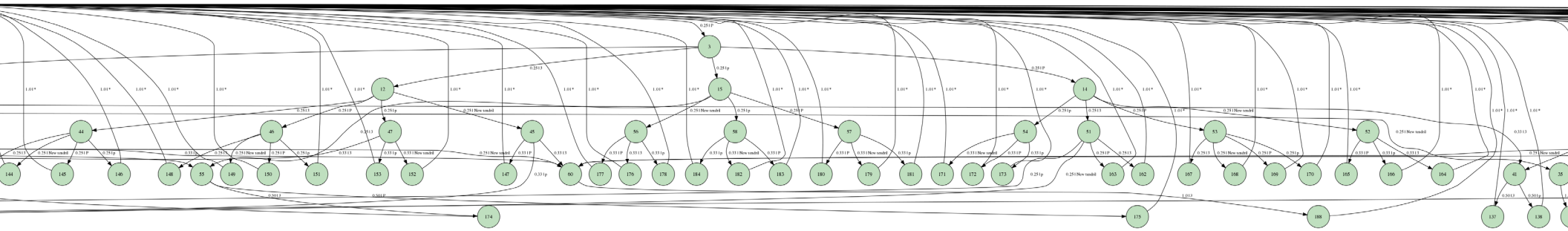

Unifilar E-Machine for Subsymbol Periodicity (“p”, “P”, “3”), Morph Length 2 (continued on next page!)

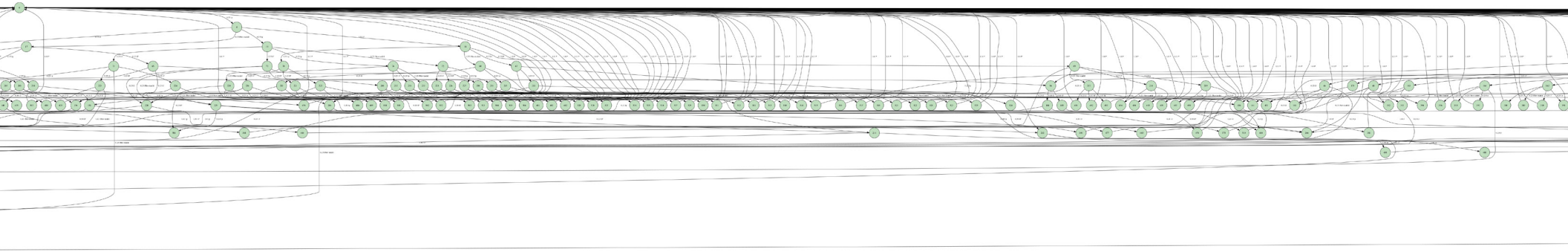

Unifilar E-Machine for Subsymbol Periodicity (“p”, “P”, “3”), Morph Length 4 (continued on next page!)

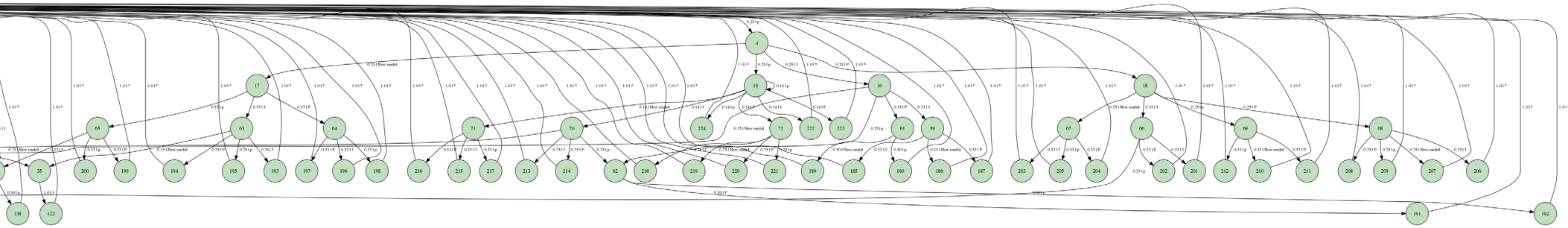

Unifilar E-Machine for Subsymbol Periodicity (“p”, “P”, “3”), Morph Length 2 (final page!)

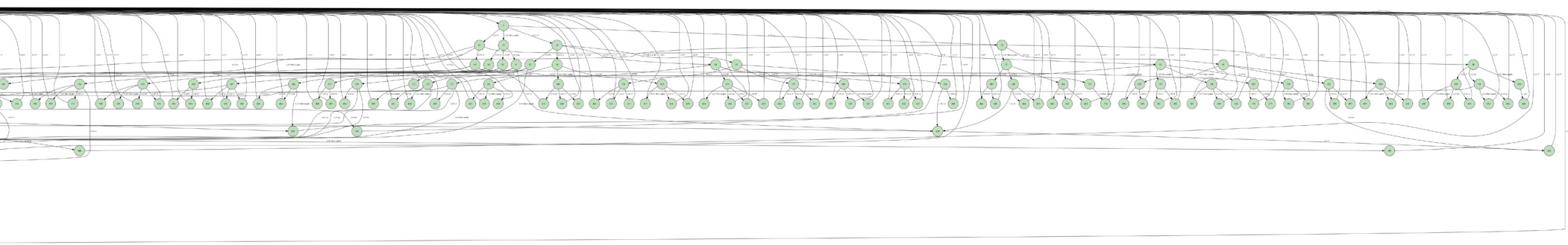

Unifilar E-Machine for Subsymbol Periodicity (“p”, “P”, “3”), Morph Length 4 (final page!)

Brief Overview of Significant Factors in Real Tendril Data

159 out of 324 (49.07%) Total Possible Symbols Have Zero Probability in our Real Tendril Data: Why?

16 Sub-symbols total, from 6 categories, combine to create each symbol: d, D, 2, p, P, 3, L, R, S, 0, 1, 4, 9, 8, c, f
[0,1,2,3,4,5] = 23S19c (example) The ones that have zero probability for the most part are these:

1) They have a "c" ("self-contact") at position 5; only 5% of our measurements have "c", so 95% don't.

2) They have an "S" ("straight") but also have a "P" (2-4 coils) or a "3" (4+ coils): straight tendrils are not coiling tendrils.

3) They have an "8" or a "9" at position 4 - only 8% of our measurements overall have an "8" (180-degree reversal), and only 15% have a "9" (90-degree turn).

4) They have a "D" or a "2" (both of which mean, fairly sizable to large coils), but also have a "P" or a "3", meaning, they have LOTS of fairly large coils. In general, our tendrils may have 1 or 2 large coils usually in isolation (one in the middle somewhere, or, at the end when it is opening out to the base). Mostly we have average to small tight coils of higher periodicity.

5) They have an "S" ("straight") but also have a "0" ("no perversion"); we very rarely used "S" when it was not also associated with a "1" ("perversion") since usually we could usually tell which way it was twisting.

Overall Entropy of 324 Symbols: 5.48981401109

Real Tendril Top Twenty:

Only 20 symbols out of 324 have a greater than 1% probability of occurrence (1.003% - 8.999%).

4 of the top 5 likely reference the number of measurements and frequency with which they occur when a tendril coil is ending, meaning, when it is widening and opening up toward the base. These are: '2pL04f', '2pR04f', 'DpL04f', 'DpR04f'. The other one in the top 5 is '2pS14f', which is the symbol that represents a perversion filling the 5mm increment.

'2pL04f', '2pR04f', 'DpL04f', 'DpR04f'

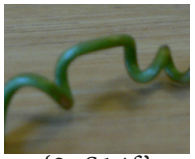

'2pS14f'

In the top 20, 14 are symbol "pairs" where they are the same symbol, just one is Left-handed and one is Right-handed. These are: '2pL04f'/ '2pR04f', 'D3L04f'/'D3R04f', 'DPL04f'/ 'DPR04f', 'DpL04f'/'DpR04f', 'd3L04f'/'d3R04f', 'dPL04f'/'dPR04f', 'dpL04f'/'dpR04f'. This reflects the high freqency of these particular symbol patterns, despite the overall difference that there are more Left-handed coils (51.73%) than Right-handed coils (38.39%).

Building a 1D Mathematical Model to Simulate Tendril Free Coiling Morphologies

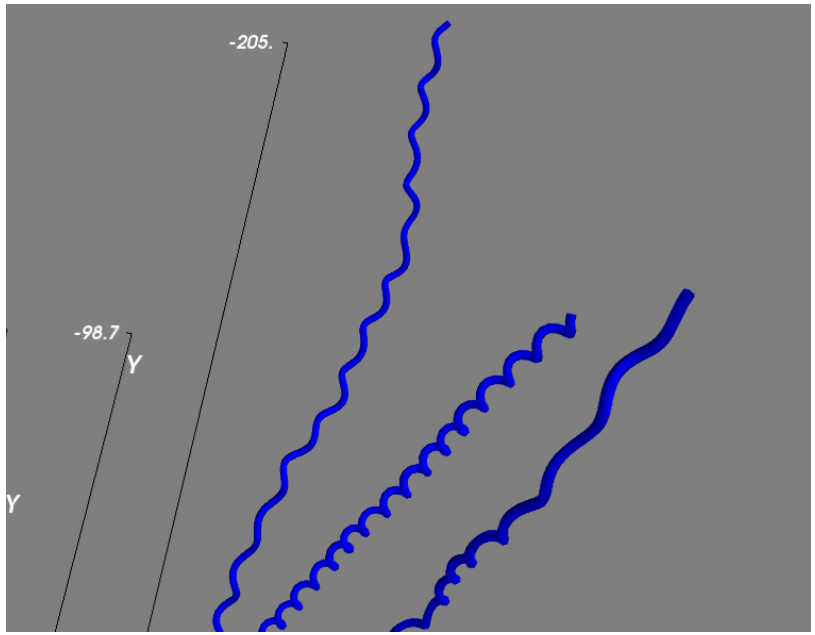

1D Turing Reaction-Diffusion Helical Model: Achieves Variation in Diameter, Periodicity and Angle Axis, but No Perversions

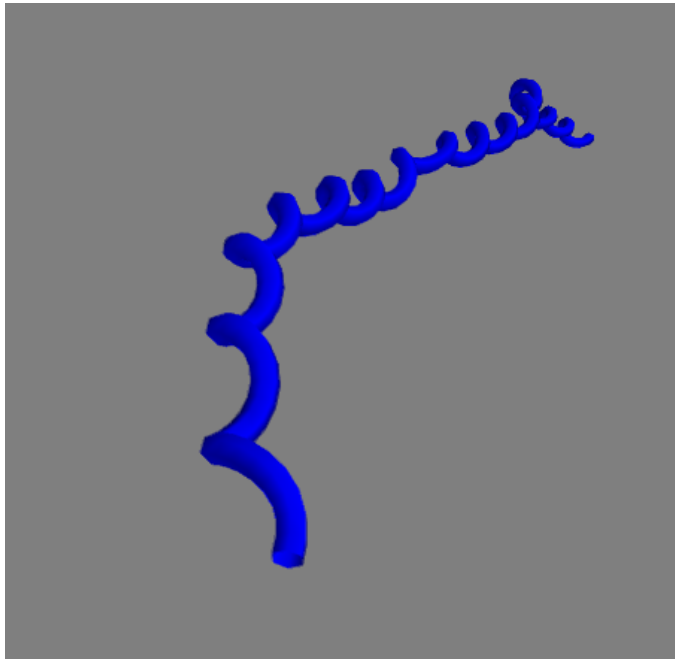

```
# Turing ODE setup:
#       Parameters:
As = .12 #.2    # Strength by which activator is induced by itself
Ad = .4 #.1     # Decay rate of activator
B  = .2 #.1?    # Intensity by which the activator is repressed by the inhibitor
C  = .1 #.07    # Strength by which inhibitor is induced by activator
D  = .09        # Decay rate of inhibitor
E  = .04        # Background rate of activator generation?
Du = .1 #1              # Diffusion coefficient for activator
Dv = .6 #6 #.4 .2       # Diffusion coefficient for inhibitor

#       ICs:
#u = zeros(Nsegments,'float')   # activator
#v = zeros(Nsegments,'float')   # inhibitor
u = 0.1*random.rand(Nsegments)  # activator
u[Nsegments/2:Nsegments] = 5*u[Nsegments/2:Nsegments]   # for assymetric IC w/ noise (greater noise w/ greater signal too)
u[175] = 1.     # for reference in figuring out spacetime map
v = 0.1*random.rand(Nsegments)  # inhibitor
```

...

```
        dudt = LinSigmoid((E + As*u - B*v),SigStart,SigEnd) -2.*Du*u + Du*(LuNeighbs + RuNeighbs)
        dvdt = C*u - D*v - 2.*Dv*v + Dv*(LvNeighbs + RvNeighbs)

        #u = u + dudt*dt
        #v = v + dvdt*dt
        u = LinSigmoid((u + dudt*dt),0,uMAX)    # shouldn't have negative u! should saturate though?...
        v = v + dvdt*dt

        if remainder(time,floor(Ntimesteps/EvStepsShown)) == 0:
                EvStep += 1
                OneDTuringEvol[EvStep,:] = u
```

...

```
# NOW translate final u to twist and bend:
#       algorithm parameters
R = 1.          # normalized radius
dL = 1.2        # in units of radius
g = 1./2.       # What are the consequences of varying this parameter?

phi1    = 23.*pi/180. #pi/2.5 #pi/8.    # More generally, could be an array, either for sweeping through a parameter or even having phi1 change throughout
the length
#theta2  = u/uMAX*thetaMAX      # now an array

#ds = sqrt(pow((dL+g*sin(theta2)),2) + pow(g*(1-cos(theta2)),2))                # assuming phi1 and theta2 are constant...

  # Initiate arrays for stored info (only really need to store x for visualization, but may be helpful to hold the d_i's for analysis)

x  = zeros((3,Nsegments),'float')       # to hold space curve,          x(s)
d1 = zeros((3,Nsegments),'float')       # tangent to space curve:       d1(s) = dx/ds
d2 = zeros((3,Nsegments),'float')       # orthonormal to d1 and d3:     d2(s) = cross(d3,d1)
d3 = zeros((3,Nsegments),'float')       # towards axis of second rotation in local basis
s  = zeros((1,Nsegments),'float')       # could just describe whole s(i) from the outset if phi1 and theta2 will be constant...

  # Initial conditions

x[:,0]  = array([0.,0.,0.])             # start @ origin
d1[:,0] = array([1.,0.,0.])             # x-hat
d2[:,0] = array([0.,1.,0.])             # y-hat
d3[:,0] = array([0.,0.,1.])             # z-hat
s[0] = 0.

  # Iterate finite difference equations
  #

for i in arange(1,Nsegments,1,'int'):

        theta2 = u[i]/uMAX*thetaMAX     # arange(1,Nsegments,1,'int') only lets i get to Nsegments-1
        ds = sqrt(pow((dL+g*sin(theta2)),2) + pow(g*(1-cos(theta2)),2))

        d1temp  = cos(phi1)*d1[:,i-1] - sin(phi1)*d2[:,i-1]     # intermediate d1 after phi1 rotation (separate step for computational ease, although coul
 be woven into the difference eqn.s directly)
        d2[:,i] = sin(phi1)*d1[:,i-1] + cos(phi1)*d2[:,i-1]     # final d2, since second rotation does not affect d2
        x[:,i]  = x[:,i-1] + g*(1-cos(theta2))*d1temp + (dL + g*sin(theta2))*d3[:,i-1]
        d3[:,i] = sin(theta2)*d1temp + cos(theta2)*d3[:,i-1]
        d1[:,i] = cos(theta2)*d1temp - sin(theta2)*d3[:,i-1]
        # above order of calculating x,d1,d2, and d3 can be interchanged; put this way for conceptual convenience
        s[0,i] = i*ds


plot3d(x[0,:].tolist(),x[1,:].tolist(),x[2,:].tolist(),s[0,:].tolist(),color=(0.,0.,1.),tube_radius=R) #0.1)
axes(color=(0.,0.,0.))
```

Turing Reaction-Diffusion Patterns across 1D Simulated Tendril: Playing with Parameters

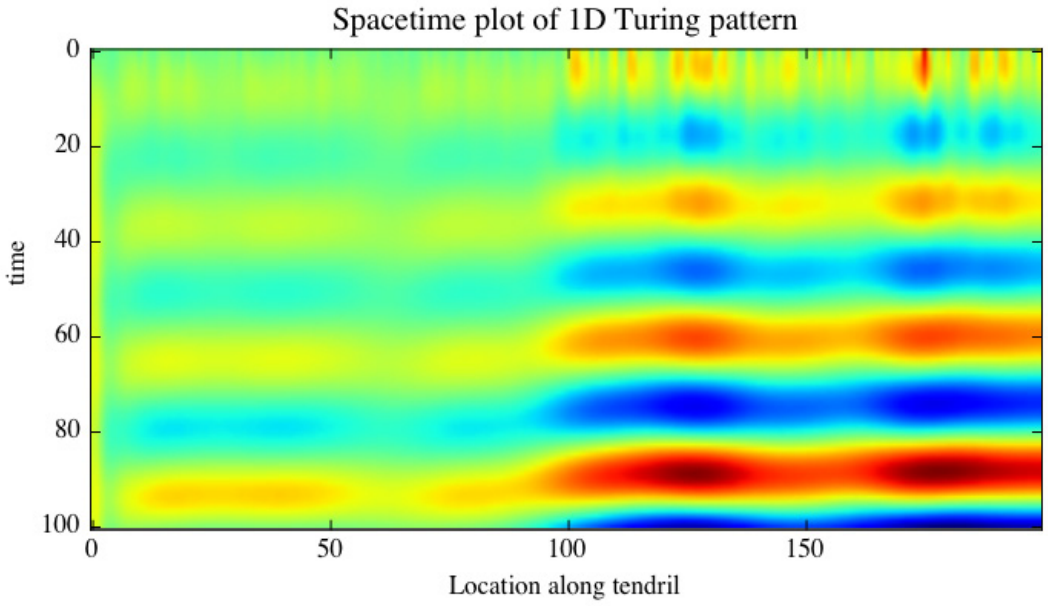

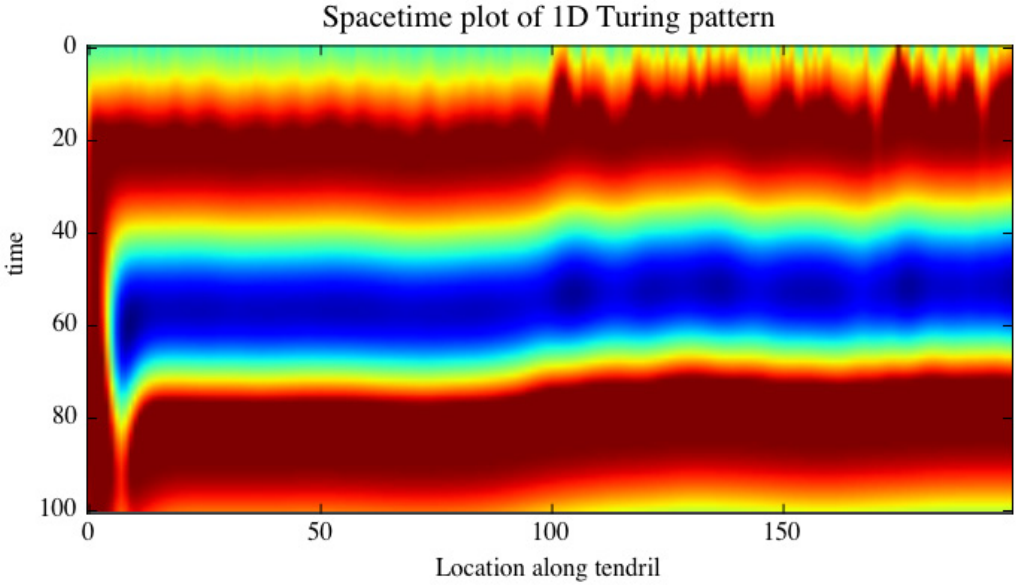

Turing Equations for Activator-Inhibitor dynamics from Fujita, Hironori et al, "Reaction-Diffusion Pattern in Shoot Apical Meristem of Plants," PLoS ONE 6:3 (2011): e18243.

The basic dynamics of the activator (u_i) and inhibitor (v_i) in the i-th cell is described by the following form of equations:

$$\frac{du_i}{dt} = \Phi(E + A_s u_i - B v_i) - A_d u_i + D_u \sum_{j=neighbors} (u_j - u_i) \quad (1a)$$

$$\frac{dv_i}{dt} = C u_i - D v_i + D_v \sum_{j=neighbors} (v_j - v_i) \quad (1b)$$

with the constraint condition in the activator synthesis (Fig. 1B),

$$\Phi(x) = \varphi(x) = \frac{A_d u_{max}}{2} \left(1 + \frac{2x/(A_d u_{max}) - 1}{\sqrt[n]{1 + |2x/(A_d u_{max}) - 1|^n}} \right) \quad (2a)$$

or

$$\Phi(x) = \phi(x) = \begin{cases} 0 & (x < 0) \\ x & (0 \le x \le A_d u_{max}) \\ A_d u_{max} & (A_d u_{max} < x) \end{cases} \quad (2b)$$

where $A_s \equiv A + A_d$, A_d, B, C, D, E, D_u, D_v, $u_{max} \equiv U_{max} u_0$, and n are positive constants, and u_0 is the equilibrium value of the activator (u_i) in a simplified form by Equations (3) without space. $\varphi(x)$ is a sigmoidal function ranged between 0 and $A_d u_{max}$ (Fig. 1B). The constraint on the activator synthesis $0 \le \Phi(x) \le A_d u_{max}$ results in that on the activator concentration $0 \le u_0 \le u_{max}$, because the equilibrium condition in Equation (1a) without space leads to the equation $u_i = \Phi(E + A_s u_i - B v_i)/A_d$. Three terms of the right hand side of Equation (1a) or (1b) represent the synthesis, degradation, and diffusion of the activator or inhibitor, respectively. That is, the activator is induced by itself in the strength A_s, is repressed by the inhibitor in the intensity of B, decays at the rate A_d, and diffuses between adjacent cells with the diffusion coefficient D_u. On the other hand, the inhibitor is induced by the activator in the strength C, decays at the rate D, and diffuses with the diffusion coefficient D_v.

Still to Come: 2D Modeling Approach for Tendril Coiling Simulation

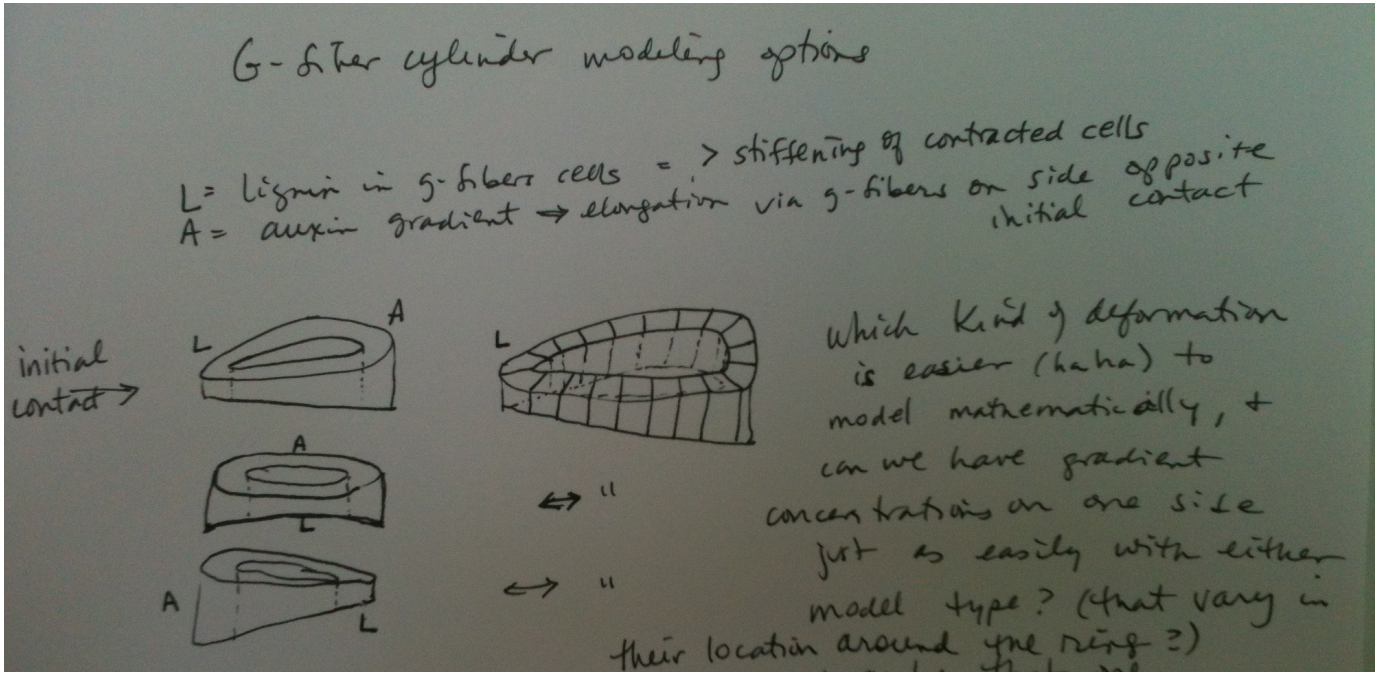

Our 2D model will unfold the tendril "cylinder" as diagrammed at the left into a 2D rectangle with gradient flow wrapping across the edges.

Gradient Flow Model:
From Contracting G-Fiber Contact Side with Lignification (L)
to Elongating High-Auxin Level Side (A) Opposite Contact

While the whole tendril coil is not a perfect example of Turing's reaction-diffusion process, auxin is "self-regulating" in that auxin-triggered genes inhibit auxin production when the auxin-triggered process is complete. In this sense, auxin is both an "Activator" and its own "Inhibitor" in Turing's reaction-diffusion equation.

Similarly, researchers hypothesize that lignin also exists in varying levels on the contact side in the g-fiber cell zone, with higher lignification zones causing greater stiffness during the contacting and twisting process.

We therefore are using reaction-diffusion equations to establish variable levels across our 2D tendril, in order to study its effectiveness in producing variable helical coiling patterns.

Our 2D mathematical model also establishes a relationship (___of some sort?____) between the elongation and contraction sides of the tendril, and a proportional relationship between auxin level and amount of elongation.

Still to Come: Constructing Epsilon-Machines of Simulated Free Coiling Tendrils

Comparison of Epsilon-Machines for Real and Simulated Tendils: What do we learn? (???????)

Final Results: Analysis of our Method and Models, and Emergent Structures in Free Coiling Tendril Nonlinear Dynamics

Bibliography

General on Vines and Tendrils

Darwin, Charles, *The Movements and Habits of Climbing Plants* (1876).

den Dubbleden, KC and B. Oosterbeek, "The Availability of External Supports Affects Allocation Patterns and Morphology of Herbaceous Climbing Plants," *Functional Ecology* 9:4 (August 1995): 628-634.

Drouin, Jean-Marc and Thierry Deroin, "Minute observations and theoretical framework of Darwin's studies on climbing plants," *C. R. Biologies* 333 (2010): 107-11.

Hofer, Julie, et al, "*Tendril-less* Regulates Tendril Formation in Pea Leaves," *The Plant Cell* 21 (February 2009): 420-28.

Jaffe, M. J. and A. W. Galston, "The Physiology of Tendrils," *Annual Review of Plant Physiology* 19 (1968): 417-34.

Jaffe, M. J., and A. W. Galston, "Physiological Studies on Pea Tendrils. V. Membrane Changes and Water Movement Associated with Contact Coiling," *Plant Physiology* 43 (1968): 537-42.

Keller, Joseph, "Tendril Shape and Lichen Growth," *Lectures on Mathematics in the Life Sciences* 13 (1980): 257-74.

MacDougal, D. T., "The Mechanism of Curvature in Tendrils," *Annals of* Botany via Oxford Journals 10:39 (Sept. 1896): 373-403.

_____, "The Tendrils of Passiflora caerulea," *Botanical Gazette* 18:4 (April 1893): 123-30.

Morris, Anne K. and Wendy K. Silk, "Use of a Flexible Logistic Function to Describe Axial Growth of Plants," *Bulletin of Mathematical Biology* 54:6 (1992): 1069-81.

Nakajima, Keiji, Tomomi Kawamura, and Takashi Hashimoto, "Role of the SPIRAL1 Gene Familly in Anisotropic Growth of *Arabidopsis thaliana*," *Plant Cell Physiology* 47:4 (2006): 513-22.

Putz, Francis and H. A. Mooney, eds., *The Biology of Vines* (1991), with a chapter on biomechamics.

Silk, Wendy K, "Growth Rate Patterns which Maintain a Helical Tissue Tube," *Journal of Theoretical Biology* 138 (1989): 311-27.

_____, "On the Curving and Twining of Stems," *Environmental and Experimental Botany* 29:1 (1989): 95-109.

Tropic Response

Carrington, CMS, and J Esnard, "Kinetics of thigmocurvature in two tendril-bearing climbers," *Plant, Cell and Environment* 12 (1989): 449-454.

Chehab, E. Wassim, Elizabeth Eich and Janet Braam, "Thigmomorphogenesis: a complex plant response to mechano-stimulation," *Journal of Experimental Botany* 60:1 (2009): 43-56.

Ding, Zhaojun et al, "Light-mediated polarization of the PIN3 auxin transporter for the phototropic response in *Arabidopsis*," *Nature Cell Biology* 13:4 (April 2011): 447-53.

Engelberth, Jurgen, "Mechanosensing and Signal Transduction in Tendrils," *Adv. Space Res.* 32:8 (2003): 1611-19.

Friml, Jiri et al, "Lateral Relocation of auxin efflux regulator PIN3 mediates tropism in *Arabidopsis*," *Nature* 415 (14 February 2002): 806-09.

Gerrath, Jean, Richard Cote, and Melissa Farquhar, "Pea (Pisum sativum L.) Tendril-Surface Changes are Correlated with Changes in Functional Development," *International Journal of Plant Sciences* Vol. 160, no. 2 (March 1999), 261-274.

Hamant, Olivier, "Developmental Patterning by Mechanical Signals in *Arabidopsis*," *Science* 322 (2008): 1650-55.

Heiser, Marcus et al, 'Alignment between PIN1 Polarity and Microtubule Orientation in the Shoot Apical Meristem Reveals a Tight Coupling between Morphogenesis and Auxin Transport," *PLOS Biology* 8:10 (October 2010): e1000516.

Jaffe, M. J. "The Role of Auxin in the Early Events of the Contact Coiling of Tendrils," *Plant Science Letters* 5 (1975): 217-25.

Junker, Steffen, "A Scanning Electron Microscopic Study on the Developmnt of Tendrils of Parthenocissus tricuspidata Sieb.& Zucc.," *New Phytologist* 77:3 (November 1976): 741-746.

_____, "Thigmonastic Coiling of Tendrils of *Passiflora quadrangularis* is Not Caused by Lateral Redistribution of Auxin," *Physiol. Plant*. 41 (1977): 51-54.

Larson, Katherine, "Circumnutation Behavior of an Exotic Honeysuckle Vine and Its Native Congener: Influence on Clonal Mobility," *American Journal of Botany* 87(4) (2000): 533-538.

Adhesion + Blep/Mechanoreceptor Cells in Tendrils

Engelberth, Jurgen, Gerhard Wanner, Beate Groth, Elmar Weiler, "Funcational Anatomy of the mechanoreceptor in tendrils of *Bryonia dioica* Jacq.," *Planta* 196 (1995): 539-550.

Bowling, A. J., and K.C. Vaughn, "Structural and immunocytochemical characterization of the adhesive tendril of Virginia Creeper," *Protoplasma* 232 (2008): 153-63.

Endress, Anton, and William Thomson, "Adhesion of the Boston Ivy Tendril," *Canadian Journal of Botany* 55 (1977): 918-924.

Gelatinous Fibers in tendrils for coiling

Bowling, Andrew and Kevin Vaughn, "Gelatinous Fibers are Widespread in Coiling Tendrils and Twining Vines," *American Journal of Botany* 96(4) (2009): 719-727.

Boyd, J. D. "Helical Fissures in Compression Wood Cells: Causative Factors and Mechanics of Development," *Wood Science and Technology* 7 (1973): 92-111.

Clair, Bruno, Bernard Thibaut, and Junji Sugiyama, "On the detachment of the gelatinous layer in tension wood fiber," *Journal of Wood Science* 51 (2005): 218-221.

Meloche, Christopher, J. Paul Knox, Kevin Vaughn, "A cortical band of gelatinous fibers causes the coiling of redvine tendrils: a model based upon cytochemical and immunocytochemical studies," *Planta* 225 (2007): 485-98.

Pilate, Gilles, et al, "Lignification and tension wood," *C. R. Biologies* 327 (2004): 889-901.
Vaughn, Kevin and Andrew Bowling, "Biology and Physiology of Vines," *Horticultural Reviews* 38 (2011): 1-21.
Yamamoto, Hiroyuki, "Role of the gelatinous layer on the origin of the physical properties of the tension wood," *Journal of Wood Science* 50 (2004): 197-208.
Yamamoto, Hiroyuki et al, "Role of the gelatinous layer (G-layer) on the origin of the physical properties of the tension wood of *Acer sieboldianum*," *Journal of Wood Science* 51 (2005): 222-33.

Physical Mechanics and Kinematic Models of Helical Structures (Tendrils, DNA, Bacillus flagella)

Aguirregabirla, J. M, A. Hernandez, and M. Rivas, "A note on the graphical representation of rotations," *Eur. J. Phys*. 13 (1982): 139-41.
Benham, Craig, and Steven Mielke, "DNA Mechanics," *Annual Review of Biomedical Engineering* 7 (2005): 21-53.
Callan-Jones, A., P. T. Brun, and B. Audoly, "Self-Similar Curling of a Naturally Curved Elastica," *Physical Review Letters* 108 (27 Apr. 2012): 174302.
Coleman, Bernard, Wilma Olson, and David Swigon, "Theory of sequence-dependent DNA elasticity," *Journal of Chmical Physics* 118:15 (15 Apr. 2003): 7127-40.
Domokos, G. and T. J. Healey, "Multiple Helical Perversions of Finite, Intrinsically Curved Rods," *International Journal of Bifurcation and Chaos* 15:3 (2005): 871-90.
Goldstein, Raymond and Alain Goriely, "Dynamic buckling of morphoelastic filaments," *Physical Review E* (2006): 010901.
Goldstein, Raymond, Alain Goriely, Greg Huber, and Charles Wolgemuth, "Bistable Helices," *Physical Review Letters* 84:7 (14 Feb. 2000): 1631-35.
Goriely, Alain, M. Nizette, and M. Tabor, "On the Dynamics of Elastic Strips," *J. of Nonlinear Science* 11 (2001): 3-45.
Goriely, Alain, and Michael Tabor, "Spontaneous Helix Hand Reversal and Tendril Perversion in Climbing Plants," *Physical Review Letters* 80:7 (16 Feb. 1998): 1564-67.
Jensen, Mari, "Mathematicians Describe Tendril Perversion," *Science News* 153:9 (28 Feb. 1998): 134.
Klapper, I., "Biological Applications of the Dynamics of Twisted Elastic Rods," *Journal of Computational Physics* 125 (1996): 325-37.
McMillen, T. and A. Goriely, "Tendril Perversion in Intrinsically Curved Rods," *J. of Nonlinear Science* 12 (2002): 241-81.
Mendelson, Neil, "Dynamics of Bacillus subtilis helical macrofiber morphogenesis: writhing, folding, close packing, and contraction," *Journal of Bacteriology* 151:1 (1982): 438-49.

Mendelson, Neil, et al, "The dynamic behavior of bacterial microfibers growing with one end prevented from rotating: variation in shaft rotation along the fiber's length, and supercoil movement on a solid surface toward the constrained end," *BMC Microbiology* 3 (2003): 18.
Raup, David, "Geometric Analysis of Shell Coiling: General Problems," *Journal of Paleontology* 40:5 (Sept. 1966): 1178-90.
Tabor, Michael and Isaac Klapper, "Dynamics of Twist and Writhe and the Modeling of Bacterial Fibers," in *Mathematical Approaches to Biomolecular Structure and Dynamics*, eds. Jill Mesirov, Klaus Schulten, and De Witt Sumners (Springer, 1996), 139-59.
Wang, Zhong Lin, "Nanostructures of Zinc Oxide," *Materials Today* (June 2004): 26-33.

Turing Reaction-Diffusion Models of Plant Morphogenesis, Chirality, and Auxin Transport

Benkova, Eva, et al, "Local, Efflux-dependent auxin gradients as a common module for plant organ formation," *Cell* 115 (26 Nov. 2003): 591-602.
Bhalero, Rishikesh and Malcolm Bennett, "The case for morphogens in plants," *Nature Cell Biology* 5:11 (November 2003): 939-42.
Fujita, Hironori et al, "Reaction-Diffusion Pattern in Shoot Apical Meristem of Plants," *PLoS ONE* 6:3 (2011): e18243.
Payne, Robert and Claire Grierson, "A Theoretical Model for ROP Localisation by Auxin in Arabidopsis Root Hair Cells," *PLoS ONE* 4:12 (2009): e8337.
Scheres, Ben and Jian Xu, "Polar auxin transport and patterning: grow with the flow," *Genes and Development* 20 (2006): 922-26.

Auxin, Lignin, and Microtubule Studies

Aloni, Roni, Marie Therese Tollier, and Bernard Monties, "The Role of Auxin and Gibberellin in Controlling Lignin Formtion in Primary Phloem Fibers and in Xylem of *Coleus blumei* Stems," *Plant Physiology* 94 (1008): 1743-47.
Benjamin, Rene, and Ben Scheres, "Auxin: The Looping Star in Plant Development," *Annual Review of Plant Biology* 59 (2008): 443-65.
Besseau, Sebastien, et al, "Flavonoid Accumulation in *Arabidopsis* Repressed in Lignin Synthesis Affects Auxin Transport and Plant Growth," *The Plant Cell* 19 (January 2007): 148-62.
Christensen, Sioux, et al, "Regulation of Auxin Response by the Protein Kinase PINOID," *Cell* 100 (18 February 2000): 469-78.
DeLong, Alison, Keithanne Mockaitis and Sioux Christensen, "Protein phosphorylation in the delivery of and response to auxin signals," *Plant Molecular Biology* 49 (2002): 285-303.
Elobeid, Mudawi, Cornelia Gobel, Ivo Feussner and Andrea Polle, "Cadmium interferes with auxin physiology and lignification in poplar," *Journal of Experimental Botany* 63:3 (2012): 1413-21.
Feraru, Elena, et al, "PIN Polarity Maintenance by the Cell Wall in *Arabidopsis*," *Current Biology* 21 (22 Feb. 2011): 338-43.

Friml, Jiri et al, "A PINOID-Dependent Binary Switch in Apical-Basal PIN Polar Targeting Directs Auxin Efflux," *Science* 306 (2004): 862-65.
Guilfoyle, Tom and Gretchen Hagen, "Auxin response factors," *Current Opinion in Plant Biology* 10 (2007): 453-60.
Kieffer, Martin, Joshua Neve and Stefan Kepinski, "Defining auxin response contexts in plant development," *Current Opinion in Plant Biology* 13 (2010): 12-20.
Korbei, Barbara and Christain Luschnig, "Cell Polarity: PIN It Down!" *Current Biology* 21:5 (2011): R197-99.
Leyser, Ottoline, "Auxin signaling: the beginning, the middle and the end," *Current Opinion in Plant Biology* 4 (2001): 382-86.
_____, "Dynamic Integration of Auxin Transport and Signalling," *Current Biology* 16 (2006): R424-433.
Nakajima, Keiji, Tomomi Kawamura and Takashi Hashimoto, "Role of the *SPIRAL1* Gene Family in Anisotropic Growth of *Arabidopsis thaliana*," *Plant Cell Physiology* 47:4 (2006): 513-22.
Quint, Marcel and William Gray, "Auxin signaling," *Current Opinion in Plant Biology* 9 (2006): 448-453.
Sauer, Michael and Jiri Friml, "Fleeting hormone cues get stabilized for plant organogenesis," *Molecular Systems Biology* 7:507 (2011): 1-3.
Tromas, Alexandre, and Catherine Perrot-Rechenmann, "Recent progress in auxin biology," *Comptes Rendus Biologies* 333 (2010): 297-306.
Vanneste, Steffen, and Jiri Friml, "Auxin: A Trigger for Change in Plant Development," *Cell* 136 (2009): 1005-16.
Vernoux, Teva, et al, "The auxin signaling network translates dynamic input into robust patterning at the shoot apex," *Molecular Systems Biology* 7:508 (2011): 1-15.
Zhang, Jing, et al, "PIN phosphorylation is sufficient to mediate PIN polarity and direct auxin transport," *PNAS* 107:2 (12 January 2010): 918-22.

Tendril Evolution

Hofer, Julie, et al, "*Tendril-less* Regulates Tendril Formation in Pea Leaves," *The Plant Cell* 21 (Feb. 2009): 420-28.
Krings, Michael, Hans Kerp, Thomas Taylor and Edith Taylor, "How Paleozoic Vines and Lianas Got off the Ground: On Scrambling and Climbing Carboniferous-Early Permian Pteridosperms," *The Botanical Review* 69(2) (2003): 204-224.

Computational Mechanics

Crutchfield, James P., "Between Order and Chaos," *Nature Physics* 8 (January 2012): 17-24.\
_____, "Is Anything Ever New? Considering Emergence," in *Complexity: Metaphors, Models, and Reality*, G. Cowan, D. Pines, and D. Melzner, editors, SFI Series in the Sciences of Complexity XIX (Addison-Wesley, Redwood City, 1994), 479-497.

Crutchfield, James P., J. D. Farmer, N. H. Packard, and R. S. Shaw, "Chaos", Scientific American 255 (1986): 46-57.

Crutchfield, James P., and D. P. Feldman, "Regularities Unseen, Randomness Observed: Levels of Entropy Convergence", *CHAOS* 13:1 (2003) 25-54.

Johnson, Benjamin, James Crutchfield, Christopher Ellison and Carl McTague, "Enumerating Finitary Processes," Santa Fe Institute Working Paper 10-11-027 (1 December 2010), at http://arxiv.org/abs/1011.0036 .

Shalizi, C. R., and J. P. Crutchfield, "Computational Mechanics: Pattern and Prediction, Structure and Simplicity", Journal of Statistical Physics **104** (2001) 819--881.

Strelioff, C.C., J.P. Crutchfield, and A. Hubler, "Inferring Markov Chains: Bayesian Estimation, Model Comparison, Entropy Rate, and Out-of-class Modeling,"